Published in final edited form as:
Cell Microbiol. 2009 July ; 11(7): 1128–1150. doi:10.1111/j.1462-5822.2009.01316.x.

Intracellular biology and virulence determinants of *Francisella tularensis* revealed by transcriptional profiling inside macrophages

Tara D. Wehrly[1,†], **Audrey Chong**[1,†], **Kimmo Virtaneva**[3], **Dan E. Sturdevant**[3], **Robert Child**[1], **Jessica A. Edwards**[1,#], **Dedeke Brouwer**[1], **Vinod Nair**[4], **Elizabeth R. Fischer**[4], **Luke Wicke**[3], **Alissa J. Curda**[3], **John J. Kupko III**[3,‡], **Craig Martens**[3], **Deborah D. Crane**[2], **Catharine M. Bosio**[2], **Stephen F. Porcella**[3], and **Jean Celli**[1,*]

[1]Tularemia Pathogenesis Section, Rocky Mountain Laboratories, National Institute of Allergy and Infectious Diseases, National Institutes of Health, Hamilton, MT 59840, USA

[2]Immunity to Pulmonary Pathogens Section, Laboratory of Intracellular Parasites, Rocky Mountain Laboratories, National Institute of Allergy and Infectious Diseases, National Institutes of Health, Hamilton, MT 59840, USA

[3]Genomics Unit, Rocky Mountain Laboratories, National Institute of Allergy and Infectious Diseases, National Institutes of Health, Hamilton, MT 59840, USA

[4]Electron Microscopy Unit, Research Technologies Section, Rocky Mountain Laboratories, National Institute of Allergy and Infectious Diseases, National Institutes of Health, Hamilton, MT 59840, USA

Summary

The highly infectious bacterium *Francisella tularensis* is a facultative intracellular pathogen, whose virulence requires proliferation inside host cells, including macrophages. Here we have performed a global transcriptional profiling of the highly virulent *F. tularensis* subsp. *tularensis* Schu S4 strain during its intracellular cycle within primary murine macrophages, to characterize its intracellular biology and identify pathogenic determinants based on their intracellular expression profiles. Phagocytosed bacteria rapidly responded to their intracellular environment and subsequently altered their transcriptional profile. Differential gene expression profiles were revealed that correlated with specific intracellular locale of the bacteria. Upregulation of general and oxidative stress response genes was a hallmark of the early phagosomal and late endosomal stages, while induction of transport and metabolic genes characterized the cytosolic replication stage. Expression of the *Francisella* Pathogenicity Island (FPI) genes, which are required for intracellular proliferation, increased during the intracellular cycle. Similarly, 27 chromosomal loci encoding putative hypothetical, secreted, outer membrane proteins or transcriptional regulators were identified as upregulated. Among these, deletion of FTT0383, FTT0369c or FTT1676 abolished the ability of Schu S4 to survive or proliferate intracellularly and cause lethality in mice, therefore identifying novel determinants of *Francisella* virulence from their intracellular expression profile.

[*]Corresponding author: Jean Celli, PhD, National Institutes of Health, National Institute of Allergy and Infectious Diseases, Laboratory of Intracellular Parasites, Rocky Mountain Laboratories, 903 South 4th Street, Hamilton, MT 59840, Phone: +1 406 375 9713, Fax: +1 406 375 9640, jcelli@niaid.nih.gov.
[†]These authors contributed equally to this work.
[#]Present address: Department of Microbiology, Ohio State University, Columbus, Ohio, USA
[‡]Present address: Institute for Systems Biology, Seattle, WA 98103, USA

Introduction

Through long-standing co-evolution with their hosts, intracellular bacterial pathogens have evolved strategies to successfully invade, survive and proliferate within mammalian host cells. Regardless of the specific pathogenic mechanisms used, the intracellular fate of these bacteria depends on a successful overriding of the host cell bactericidal mechanisms. This is achieved via the timely expression and/or activation of dedicated virulence factors, a result of the remarkable ability of bacteria to sense their intracellular environment and respond accordingly through the induction of appropriate genes. Examples in intracellular pathogens include genes encoding the Type III secretion system-2 (T3SS-2) of *Salmonella enterica* serovar Typhimurium or the VirB Type IV secretion system of *Brucella* species, which are both induced intracellularly upon acidification of the pathogen-containing vacuole (Boschiroli *et al.*, 2002, Sieira *et al.*, 2004, Starr *et al.*, 2008, Valdivia *et al.*, 1996) and required for intracellular survival and replication (Hensel *et al.*, 1998, O'Callaghan *et al.*, 1999, Sieira *et al.*, 2000). Recent advances in RNA isolation techniques and DNA microarray technologies have allowed global transcriptional profiling of intracellular bacteria, such as *S*. Typhimurium (Eriksson *et al.*, 2003, Hautefort *et al.*, 2008), *S*. Typhi (Faucher *et al.*, 2006), *Shigella flexneri* (Lucchini *et al.*, 2005), *Mycobacterium tuberculosis* (Fontan *et al.*, 2008, Schnappinger *et al.*, 2003), *Chlamydia trachomatis* (Belland *et al.*, 2003) *Listeria monocytogenes* (Chatterjee *et al.*, 2006) and *Bacillus anthracis* (Bergman *et al.*, 2007), bringing insight into the global responses of these pathogens to their respective intracellular environments. Additionally, some of these studies combined with mutagenesis approaches have identified novel genes involved in intracellular growth (Bergman *et al.*, 2007, Chatterjee *et al.*, 2006), indicating that the intracellular induction of specific bacterial genes can serve as a clue to identify genetic determinants of pathogenesis.

Francisella tularensis is a highly infectious, Gram-negative, facultative intracellular bacterium that causes tularemia, a widespread zoonosis that affects humans. Human tularemia is a fulminating disease that can be caused by exposure to as few as 10 bacteria, the pneumonic form of which can lead to up to 25% mortality if untreated (Oyston *et al.*, 2004). Four subspecies of *F. tularensis*, *F. tularensis* subsp. *tularensis* (Type A), *F. tularensis* subsp. *holarctica* (Type B), *F. tularensis* subsp. *novicida*, and *F. tularensis* subsp. *mediasiatica* are recognized, among which strains from subspecies *tularensis* and *holarctica* can cause tularemia in humans (Ellis *et al.*, 2002). Type A strains, which are geographically distributed in North America, are highly virulent and account for the most severe cases of the disease. As a facultative intracellular pathogen, *F. tularensis* is capable of infecting and proliferating in a variety of host cell types, including hepatocytes, endothelial cells, fibroblasts, and mononuclear phagocytes (Ellis *et al.*, 2002). Macrophages are believed to be an important target for infection *in vivo*, and the pathogenesis of *F. tularensis* depends on the bacterium's ability to survive and replicate within these host cells (Ellis *et al.*, 2002). Various models of *Francisella*-macrophage interactions using either virulent, attenuated or non-human pathogenic strains, and murine or human macrophages or macrophage-like cell lines, have been developed to characterize the intracellular cycle of this bacterium (Checroun *et al.*, 2006, Clemens *et al.*, 2004, Golovliov *et al.*, 2003, Santic *et al.*, 2005a, Schulert *et al.*, 2006). Although the disparity of these models may have generated controversial findings about the timing of intracellular events (Checroun *et al.*, 2006, Clemens *et al.*, 2004, Santic *et al.*, 2005a), a consensual model is that *F. tularensis* survival and replication inside macrophages relies upon its ability to escape from its initial phagosome and reach the cytosol where it extensively replicates. Following replication, the Live Vaccine Strain (LVS), an attenuated Type B derivative, and virulent Type A and Type B strains can reenter the endocytic compartment of murine primary macrophages to reside within large fusogenic vacuoles that display autophagic features (Checroun *et al.*, 2006). Altogether, our current understanding of the *Francisella* intracellular cycle indicates that

this pathogen trafficks through various intracellular compartments where it is likely subjected to different environmental cues.

Some genetic determinants of *Francisella* intracellular growth have been identified using random transposon mutagenesis and loss of function screens in various host cells (Gray *et al.*, 2002, Maier *et al.*, 2007, Qin *et al.*, 2006, Tempel *et al.*, 2006), or through differential expression analysis of genes regulated *in vitro* by the *Francisella* virulence regulator MglA (Baron *et al.*, 1998, Lauriano *et al.*, 2004, Brotcke *et al.*, 2008, Brotcke *et al.*, 2006). Additionally, *in vivo* screens for transposon insertional mutants defective for virulence have also identified genes involved in intracellular growth (Su *et al.*, 2007, Weiss *et al.*, 2007), illustrating how essential intracellular proliferation is to *Francisella* global virulence. A prominent locus required for intracellular growth is the *Francisella* Pathogenicity Island (FPI, Fig. 4A), a ~ 30-kb region that potentially encodes a secretion system (Nano *et al.*, 2004, de Bruin *et al.*, 2007) similar to the recently identified Type 6 secretion systems (T6SS) (Mougous *et al.*, 2006, Pukatzki *et al.*, 2006). This suggests that *Francisella* expresses specialized machineries to secrete proteins either to the bacterial surface or into the host cell, but such effectors of intracellular pathogenesis have not yet been identified. Nevertheless, functions encoded by the FPI have been associated with phagosomal escape and intracellular growth, since insertional or deletion mutants in *iglA* and *iglB* (Gray *et al.*, 2002), *iglC* (Golovliov *et al.*, 2003, Lauriano *et al.*, 2003, Santic *et al.*, 2005b), and *pdpA* (Nano *et al.*, 2004), are defective for intramacrophage growth, and *iglC* mutants in *novicida* and *holarctica* LVS strains are defective in phagosomal escape (Lindgren *et al.*, 2004, Santic *et al.*, 2005b, Chong *et al.*, 2008). This indicates that IglC-dependent FPI-encoded functions are involved in the early stages of *Francisella* intracellular trafficking.

Although genetic screens have proven valuable to identify the FPI (Gray *et al.*, 2002, Nano *et al.*, 2004), novel virulence genes (Brotcke *et al.*, 2006) or specific *F. novicida* genes that modulate the host ASC/Caspase 1 cell death pathway (Weiss *et al.*, 2007), much remains to be understood about the bacterial determinants of *Francisella* pathogenesis. Specifically, little is known about the intracellular biology of this bacterium and the specific genes it requires to ensure its intracellular survival and proliferation. Because *Francisella* likely responds to its intracellular environment by temporally expressing virulence factors during its intracellular cycle, we have postulated that genes required for intracellular pathogenesis and global virulence can be identified based on their increased expression inside macrophages. We have therefore performed the transcriptional profiling of intracellular virulent Type A *Francisella* during its infection cycle within murine bone marrow derived macrophages to globally identify genes that are upregulated intracellularly. Here we report a combination of genomics, cell biological and genetic approaches that have identified novel virulence factors of *Francisella* based on their intracellular expression, and characterized the intramacrophage biology of this highly infectious bacterium.

Results and Discussion

Intracellular cycle of virulent *F. tularensis* strain Schu S4 in murine bone marrow-derived macrophages

In order to perform relevant and meaningful transcriptional profiling of intracellular *F. tularensis*, it was necessary to first characterize the *Francisella*-macrophage interaction model we selected. In particular, detailing the timing of the bacterium's intracellular cycle was important to the experimental design of the transcriptional analysis. In this study, we used a model of primary murine bone marrow-derived macrophage (BMMs) infection with *F. tularensis* subsp. *tularensis* strain Schu S4, a prototypical highly virulent Type A strain whose genome has been sequenced (Larsson *et al.*, 2005). In synchronized infections of BMMs, we examined the kinetics of phagosomal disruption using a phagosomal integrity

assay (Checroun *et al.*, 2006), quantified intracellular growth, and analyzed the overall intracellular cycle by confocal and transmission electron microscopy. As previously observed with the *F. tularensis* subsp. *holarctica* strain LVS in BMMs (Checroun *et al.*, 2006), internalized Schu S4 were rapidly accessible to cytoplasmically delivered anti-*Francisella* LPS antibodies (Fig. 1A), demonstrating a rapid disruption of the *Francisella*-containing phagosome (FCP). While half of the bacteria remained enclosed within phagosomes at 30 min post infection (p.i., Fig. 1A and B), the majority of them had disrupted their phagosomal membrane at 1 h p.i. (73 ± 6.3%; Fig. 1A and C). By 4 h p.i., all bacteria were cytosolic and displayed patterns of initial replication (Fig. 1A and D). From 4 to 16 h p.i., Schu S4 underwent extensive cytosolic replication (Fig. 1A and E-F), with a maximal growth rate between 8 and 12 h p.i.. At that time, Schu S4 intracellular doubling time (53 ± 1.0 min, data not shown) significantly exceeded those of the virulent Type B strain FSC200 (109 ± 24 min, data not shown) or LVS (114 ± 4 min, data not shown), suggesting that highly virulent Type A strains exhibit higher intracellular fitness than less virulent or attenuated Type B strains. After 16 h p.i., intracellular growth stalled (Fig. 1A) and bacteria were found within late endosomal vacuoles characterized by LAMP-1-positive membranes and ultrastructural features of autophagic vacuoles (Fig. 1G), known as *Francisella*-containing vacuoles (FCVs) (Checroun *et al.*, 2006). Hence, the intracellular cycle of Schu S4 in BMMs includes an early phagosomal stage up to 1h p.i., a lag phase in the cytosol, between 1 and 4 h p.i., a stage of extensive cytosolic proliferation between 4 and 16 h pi, and a late vacuolar stage between 16 and 24 h p.i.

Transcriptional profiling of intracellular Schu S4

Because of the variety of the intracellular stages in the cycle of *Francisella* inside macrophages, we postulated that the bacterium expresses various subsets of genes at specific stages. In an attempt to comprehend gene expression changes along the entire *Francisella* intracellular cycle, our experimental design included time points encompassing all intracellular stages, namely 1, 2, 4, 8, 12, 16 and 24 h p.i. Additionally, a time zero sample corresponding to the immediate processing of bacteria added directly to BMMs was generated to obtain initial bacterial expression profiles as a baseline for identification of genes upregulated within macrophages. BMMs were infected as described in the Materials and Methods section and samples were collected for total RNA isolation according to a predesigned randomization scheme. RNA isolation yielded high quality RNA, with detectable bacterial ribosomal RNAs in samples containing high numbers of bacteria (0, 12, 16 and 24 h p.i.; Fig. 2A). Because the amount of bacterial RNA in samples containing limited numbers of bacteria (1, 2, 4 and 8 h p.i.; Fig. 2A) was not sufficient (< 1 μg) to generate exploitable microarray data, all total RNA samples were subjected to an RNA amplification step, as described in the Materials and Methods section, which generated sufficient amounts of complementary RNA (cRNA) targets to proceed with hybridization on Affymetrix DNA custom GeneChip arrays. Analyses of the microarray data (GEO series number GSE12663) using either a Pearson correlation similarity measure (not shown) or quantile normalization without background correction (PCA plot, Fig. 2B) showed that whole genome expression profiles from biological replicates clustered according to time points (Fig. 2A), therefore validating our experimental design. Interestingly, distances between sample clusters within the PCA plot revealed important changes in gene expression between time zero and 1 h p.i., indicating a significant response of *Francisella* during the early phagosomal stage. Despite clustering separately, global gene expression profiles at 1 h and 2 h p.i. and at 8 and 12 h p.i., respectively, were similar (Fig. 2A), consistent with the specific intracellular stages of entry into the cytosol and extensive cytosolic replication, respectively (Fig. 1). Global expression profiles at 4, 16 and 24 h p.i. all appeared unique and likely represented the onset of intracellular growth (4 h p.i.), the transition towards FCV formation (16 h p.i.), and the late vacuolar stage (24 h p.i.), respectively. Overall, there was

a temporal correlation between global gene expression profiles and specific intracellular stages, strongly suggesting that *Francisella* alters its transcriptional profile according to its intracellular location.

To further analyze *Francisella* expression profiles and identify genes upregulated during the intracellular cycle, signals from each gene probe set at each time point were normalized to those at time zero to generate heat maps of mRNA fold changes and reveal intracellular expression profiles of individual genes (Supplementary Material, Fig. S1). A two-fold change cut-off was used to define significant up- or down-regulation of a gene compared to its level at time zero. While a relatively constant number of genes were downregulated, ranging from 121 at 1 h p.i. to 183 at 12 h p.i. (Fig. 2C), the number of genes showing a significant upregulation increased over time, ranging from 78 at 2 h p.i. to 257 at 24h p.i., indicating an increasing response of *Francisella* to its intracellular environment. Over the whole time course, 658 genes showed significant changes in their expression, among which 298 were upregulated and 360 were downregulated (Fig. 2D). We defined an index of change in mRNA level (Fig. 2D) as the number of time points where significant changes in the expression of a particular gene were detected (Fig. 2D). Since most intracellular stages were represented in our experimental design through several time points, with the exception of the early phagosomal stage, we reasoned that genes exhibiting significant intracellular expression changes have an mRNA change index > 2. Additionally, genes showing unidirectional changes in expression over two consecutive time points (mRNA change index = 2) encompassing a particular intracellular stage were also retained for further consideration. Using these criteria, 111 genes with a mRNA change index ≥ 3 were upregulated, while 156 genes were downregulated (Fig. 2D). Further screening of the microarray data for genes showing either consistent increased expression over several consecutive time points and/or an expression profile coherent with the timing of specific intracellular stages identified a total of 152 genes that displayed expression profiles of significant upregulation within BMMs and 99 genes that were significantly downregulated (Supplementary Material, Table S1). Interestingly, various expression profiles were identified, showing significant upregulation either at all time points, during phagosomal and late vacuolar stages, or during the cytosolic replication stages. In order to examine the biological relevance of these findings, gene functions associated with these particular expression patterns were further analyzed.

Upregulation of stress response genes characterizes *Francisella* endosomal stages

Francisella genes that were most upregulated inside BMMs belonged to the general stress response pathway (Fig. 3A and Supplementary Material, Table S1). Genes encoding molecular chaperones and general stress proteins such as HtpG (FTT0356), ClpP (FTT0624), ClpX (FTT0625), the Lon protease (FTT0626), HslU (FTT0687c), HslV (FTT0688c), HtpX (FTT0862c), DnaJ (FTT1268c), DnaK (FTT1269c), GrpE (FTT1270c), a DnaJ-like chaperone (FTT1512c), GroEL/ES (FTT1696/1695), ClpB (FTT1769c) and Hsp (FTT1794) exhibited increased expression inside BMMs compared to their mRNA levels at time zero. Interestingly, most of these genes displayed a similar expression profile, with an early induction by 1 h p.i., followed by a second upregulation at 16 and 24 h p.i. (Fig. 3A). Such a remarkable expression profile was independently confirmed by quantitative PCR on *clpB* mRNA (Fig. 3D), therefore validating the microarray results. Because the highest mRNA levels of these genes corresponded to both the early phagosomal and late vacuolar stages of the *Francisella* intracellular cycle, this indicates that the early FCP and the late FCV subject *Francisella* to physiological stress, which the bacterium efficiently responds to in a coordinated manner. This genetic response is consistent with the rapid acidification of early phagosomes observed in *F. novicida*-infected human macrophages (Santic *et al.*, 2008)

and Schu S4-infected BMMs (Chong *et al.*, 2008) and the fusogenic characteristics of late vacuoles (Checroun *et al.*, 2006).

Not only general stress response genes were upregulated inside BMMs, but genes associated with oxidative stress response were significantly induced within 1 h p.i. and thereafter (Fig. 3B). These included genes encoding a Dyp-type peroxidase (FTT0086), HemC (FTT0259), glutaredoxins (FTT0533c and FTT0555), a peroxiredoxin (FTT0557), a short chain dehydrogenase (FTT0558), the methionine sulfoxide reductases MsrB (FTT0878c) and MsrA (FTT1105c, FTT1797c) and the superoxide dismutase SodC (FTT0879). While most of these genes were upregulated at 1 and 2 h p.i., only *msrA1*, *msrB* and *sodC* were also strongly upregulated at late stages (Fig. 3B), indicating that the temporal response to oxidative stress slightly differs from the general stress response. The early induction of these genes suggests the presence of oxidative stress in the early phagosome, possibly via the generation of reactive oxygen species (ROS). This is however inconsistent with the finding that LVS inhibits NADPH oxidase assembly and ROS production in human neutrophils (McCaffrey *et al.*, 2006). Provided that the same phenomenon occurs in Schu S4-infected BMMs, it remains possible that oxidative stress response genes are either upregulated through the sensing of very low levels of ROS or of other intraphagosomal cues, such as cationic antimicrobial peptides that can induce oxidative stress response genes in *S.* Typhimurium (Bader *et al.*, 2003). This would allow bacteria to consequently express redundant protective functions in addition to mechanisms of inhibition of ROS production. With such attributes, one would expect that intracellular survival of virulent *Francisella* is not affected by ROS. This hypothesis is in agreement with studies suggesting that *Francisella* killing by IFNγ-activated peritoneal exudate cells depends upon reactive nitrogen species (RNS) rather than ROS production (Lindgren *et al.*, 2007,Lindgren *et al.*, 2005). Lindgren *et al.* also examined the role of the catalase/peroxidase KatG in Schu S4 resistance to reactive species and concluded that it does not play a role in this particular strain (Lindgren *et al.*, 2007). Compared to other oxidative stress response genes, *katG* (FTT0721c) did not show any upregulation and instead was downregulated from 4 h pi. and onwards (Supplementary Material, Table S1). In spite of its secretion by intracellular bacteria in monocytes (Lee *et al.*, 2006), this enzyme does not seem to play a major role in counteracting any intracellular oxidative stress. Instead, the remarkable upregulation of other oxidative stress response genes we have identified points towards an intracellular role for these enzymes. Overall, our results demonstrate that Schu S4 efficiently responds to intracellular stress by coordinately expressing stress response genes during both the early and late endosomal stages of its intracellular cycle.

Francisella metabolism during cytosolic replication

In addition to the expression profiles of stress-related genes, a significant number of genes exhibited expression profiles of upregulation at consecutive time points between 4 and 16 h p.i., that is during the cytosolic replication stage (Supplementary Material, Table S1). Expectedly, these included genes that belong to functional categories consistent with bacterial growth, such as *de novo* nucleotide synthesis (FTT0113, FTT0114, FTT0117, FTT1229), metabolism of vitamins and cofactors (FTT1389-1391), amino acids (Fig. 4), translation and protein biosynthesis (FTT0226, FTT0228, FTT0333, FTT0334, FTT0344, FTT0403), polyamine biosynthesis (FTT0431-0435) and cell division (FTT0697, FTT1635c). Upregulated genes encoding functions related to carbohydrate metabolism (FTT0080, FTT0414, FTT0417, FTT1295c, FTT1365c, FTT1367c and FTT1483c) pointed towards the use of both glycolysis and the pentose phosphate pathway for energy metabolism. Genes encoding various transporters, such as ABC transporters (FTT0209, FTT1124, FTT1125), MFS superfamily transporters (FTT708), oligopeptide transporters (FTT0572, FTT0688c, FTT0953, FTT1233c, FTT1253) and others (FTT0175c, FTT0598c,

FTT0668), were also upregulated (Supplementary Material, Table S1), suggesting that replicating bacteria are characterized by enhanced nutrient acquisition capacities. In particular, the *fslABCDE* genes (FTT0025c-FTT0029c) (Ramakrishnan *et al.*, 2008, Sullivan *et al.*, 2006), or *figABCDE* genes in *F. novicida* (Kiss *et al.*, 2008), were highly upregulated between 4 and 12 h p.i. (Fig. 3C). These genes encode a siderophore biosynthesis and transport system that is essential for *in vitro* growth in iron-depleted conditions (Ramakrishnan *et al.*, 2008, Sullivan *et al.*, 2006) and for LVS and *F. novicida* virulence (Su *et al.*, 2007, Weiss *et al.*, 2007), but no data is available on an intracellular role. The significant upregulation of this operon during the cytosolic replication phase (from 4 to 12 h p.i., Fig. 3C) of Schu S4 strongly suggests *Francisella* enhances iron acquisition during intracellular proliferation. Because the *fsl* genes are induced under iron-limiting conditions through their regulation by Fur (Ramakrishnan *et al.*, 2008), their expression profile is consistent with restricted iron availability inside the mammalian cytosol (Shi *et al.*, 2008, Lucchini *et al.*, 2005) and illustrates *Francisella* adaptation to the cytosolic environment.

The majority of the metabolic genes upregulated intracellularly encoded functions associated with amino acid catabolism (Fig. 4A), including polyamine biosynthesis from L-arginine through spermidine (Fig. 4A), indicating that amino acids constitute a major source of nitrogen for intracellular *Francisella*. Amino acids availability likely results not only from the cytosolic pool of amino acids but also from uptake of oligopeptides, as Schu S4 remarkably encodes 8 di-/tripeptide transporters, 5 of which (FTT0572, FTT0686c, FTT0953c, FTT1233c and FTT1353) were upregulated intracellularly (Fig. 4B). Consistently, both a Xaa-Pro aminopeptidase (FTT0609) and the oligopeptidase A PrlC (FTT0899c) were upregulated inside BMMs. Taken together this indicates that Schu S4 has the capacity to transport and degrade oligopeptides during its infection cycle. Another oligopeptide transport system, the Opp ABC transporter, which is regulated in *F. novicida* by MglA but appears to downmodulate intracellular growth (Brotcke *et al.*, 2006), is likely non functional in Schu S4, since the subunits OppB and OppC-encoding genes FTT0123 and FTT0124 are truncated. Consistently, the OppD and OppF subunits-encoding genes FTT0125 and FTT0126 did not generate any detectable transcripts at any time point analyzed (data not shown).

Downregulated genes and *Francisella* intracellular adaptation

Although our study mostly focused on genes upregulated intracellularly, we also identified 99 genes with expression profiles of significant downregulation inside BMMs (Supplementary Material, Table S1). They encoded functions associated with DNA replication, transcription and translation (Supplementary Material, Table S1), indicating some alteration of *Francisella* nucleic acid metabolism and information processing in macrophages compared to *in vitro* growth conditions (time zero). Consistently, the RNA polymerase sigma-32 factor RpoH (FTT1112) was strongly downregulated while the RNA polymerase sigma-70 factor RpoD (FTT1035c) showed an early intracellular upregulation (Supplementary Material, Table S1), indicating a significant switch in gene expression following uptake by BMMs. Additionally, genes involved in either LPS (FTT0231c, FTT0232c, FTT1046c, FTT1305c) or polyglutamate capsule biosynthesis (FTT0805 and FTT0806) were downregulated within BMMs, suggesting alterations of major bacterial surface components following the transition from an extracellular to an intracellular stage. Genes encoding various transport systems, such as MFS superfamily permeases (FTT0442, FTT0446, FTT487, FTT488c), ion transporters (FTT0676, FTT1145, FTT1277c), multidrug resistance proteins (FTT1256, FTT1399, FTT1654, FTT1727c) and others (FTT0804, FTT0446) were downregulated (Supplementary Material, Table S1). Together with the intracellular upregulation of genes encoding other transporters (Supplementary Material, Table S1), these results clearly indicate significant changes in the physiology of *Francisella*

following uptake and further illustrate its adaptability to the macrophage environment. Concluding that these downregulated genes are not required for intracellular growth needs to be cautiously assessed, since one has to consider that the observed decrease in mRNA levels of these genes is relative to their expression levels in *in vitro*-grown bacteria, where they may have been upregulated on CHAB above levels required to achieve any potential intracellular functions. Indeed, 10 genes that we found to be downregulated in our analysis have been identified independently using transposon mutagenesis approaches in either LVS or *F. novicida* as being required for intracellular growth and/or virulence (Table 1). For example, the *capB* and *capC* genes (FTT0805 and FTT0806) encode functions associated with polyglutamate capsule biosynthesis and are required for intracellular growth of LVS in J774 cells (Maier *et al.*, 2007) and virulence of LVS (Su *et al.*, 2007) and *F. novicida* (Weiss *et al.*, 2007) in mice, yet these genes were downregulated inside BMMs (Supplementary Material, Table S1 and Table 1). Future studies on the roles of this putative *Francisella* capsule will clarify whether it plays a role in intracellular proliferation.

Upregulation of *Francisella* virulence determinants inside macrophages

A major goal of our transcriptional analysis of intracellular *Francisella* was to identify genes required for pathogenesis based on their expression profiles. A more detailed analysis of the microarray data showed that 39 of the 152 genes (26%) significantly upregulated inside BMMs have been previously characterized as required for intracellular proliferation and/or virulence, through transposon mutagenesis-based approaches (Table 1). They included the iron acquisition genes *fslABC*, the stress response genes *clpP, clpX, lon, dnaK, groEL* and *clpB*, genes involved in amino acid metabolism (*gcvTHP1, aspC1, metNIQ*) and several FPI genes (Table 1). This demonstrates that *Francisella* virulence determinants are induced intracellularly. We further examined the transcriptional patterns of the FPI genes (Fig. 5A), which have been identified as required for intracellular growth and virulence (de Bruin *et al.*, 2007,Gray *et al.*, 2002,Lai *et al.*, 2004,Maier *et al.*, 2007,Nano *et al.*, 2004,Santic *et al.*, 2005b,Su *et al.*, 2007,Tempel *et al.*, 2006,Weiss *et al.*, 2007). *PdpA, pdpB, dotU, iglI, pdpD* and *iglABCD* displayed significant upregulation inside BMMs (Fig. 5B), while most other FPI genes exhibited a similar expression profile, albeit below the 2-fold cut-off value for statistical significance (Fig. 5B). Although several of the FPI genes showed a rapid upregulation within the first hour p.i., maximal mRNA levels were reached by the end of the cytosolic replication stage, i.e. between 12 and 16 h p.i. (Fig. 5B). To independently validate these expression profiles, the mRNA levels of *pdpD, iglA, iglC, pdpA* and *pdpC* were measured using quantitative PCR and normalized to *gyrA* (FTT1575c) mRNA levels, which we found to be constitutively expressed at all time points (data not shown). The expression profiles of these 5 genes correlated with those obtained through microarray analysis (Fig. 5B and 6A). While *pdpC* was globally down regulated compared to time zero, *pdpD, iglA, iglC, pdpA* were upregulated and displayed a comparable expression profile, with a rapid upregulation followed by a strong increase in mRNA levels between 12 and 16 h p.i. (Fig. 6A). This indicates a coordinated regulation of all FPI transcriptional units within the FPI. *IglC* mRNA levels were much higher than those of the other FPI genes tested, suggesting a higher transcription of this gene, or increased stability of its mRNA. Although further transcriptional analysis is required to understand the expression differences in this region of the FPI, these results are consistent with IglC being prominently expressed by LVS in macrophages (Golovliov *et al.*, 1997) and by virulent Type A bacteria recovered from infected mouse spleens (Twine *et al.*, 2006). To further validate our data, we examined the intrabacterial levels of the IglC and PdpC proteins during Schu S4 intracellular cycle. While PdpC levels did not dramatically change over the whole time course, IglC intrabacterial levels increased from 0 to 4 h p.i. (Fig. 6B), further demonstrating intracellular induction of this protein (Chong *et al.*, 2008). This initial increase was later followed by a secondary accumulation visible at 24 h p.i. (Fig. 6B), consistent with the expression profiles of *iglC*

(Fig. 5B and 6A). Altogether, these results demonstrate the intracellular induction of FPI genes and validate our original assumption that genes involved in intracellular pathogenesis can be identified based on their intracellular expression profile. Through mutational analyses, functions associated with the FPI-encoded type VI secretion system have been assigned to early intracellular events, such as phagosomal escape (Lindgren *et al.*, 2004,Santic *et al.*, 2005b), implying that FPI genes must be induced rapidly upon entry. Our results corroborate these previous data by showing a rapid increase in FPI mRNA and protein levels. However, the finding that maximal expression of FPI genes takes place at the end of the cytosolic replication stage strongly argues for an additional requirement of FPI functions at later stages of the intracellular cycle.

Intracellular upregulation of genes encoding hypothetical functions

Among genes displaying significant upregulation inside BMMs, 27 encoded hypothetical proteins (Supplementary Material, Table S1), most of which do not share any significant homology with any proteins and therefore appear to be rather specific to the *Francisella* genus. These include FTT0254c, FTT0297, FTT0383, FTT1536c, FTT1541c, FTT1586c, FTT1676 and FTT1771 (Supplementary Material, Table S1 and Fig. 7A). Upregulated genes encoding proteins with putative functions were also identified, such as a Sel1 family tetratricopeptide repeat-containing protein (FTT0369c), a putative secreted transglutaminase (FTT0989), a putative outer membrane protein Omp 26 (FTT1542c), and a homolog of the *Bordetella pertussis* Bvg Accessory Factor (FTT1392) (Supplementary Material, Table S1 and Fig. 7A). Hence, putative secreted proteins, outer membrane components and transcriptional regulators were induced during the intracellular cycle, a set of bacterial factors consistent with changes in gene regulation and molecular interactions with the host cell. Although all upregulated inside BMMs, these genes exhibited differential expression profiles, suggesting that their functions are required at various stages of Schu S4 intracellular cycle. Expression of FTT0989 was maximal during the cytosolic replication stages (Fig. 7A and B), while that of FTT1542c and FTT1392 peaked at both early and late stages of the cycle (Fig. 7A and B). Interestingly, one third of these genes have been shown to be regulated by the global virulence regulator MglA in *F. novicida* (Brotcke *et al.*, 2006), a high percentage given that only 27 among the 152 genes (18%) we found to be significantly upregulated inside BMMs (Supplementary Material, Table S1) are MglA-regulated in *F. novicida* (Brotcke *et al.*, 2006). Given the prominent role of MglA in regulating virulence-associated functions in *Francisella*, this suggests that these hypothetical proteins encode pathogenesis-related functions, which is supported by the evidence that disruption of the FTT0989 locus in *F. novicida* results in decreased intracellular growth, cytotoxicity and a slight attenuation *in vivo* (Brotcke *et al.*, 2006).

Gene expression profiling identifies novel factors of intracellular survival and proliferation

To examine whether we could identify novel virulence determinants of *Francisella* through transcriptional profiling, we generated deletions of 10 upregulated loci encoding hypothetical functions (FTT0254c, FTT0297, FTT0369c, FTT0383, FTT0989, FTT1333c, FTT1392, FTT1542c, FTT1586c and FTT1676) and tested the resulting mutants for intracellular defects. We first designed and constructed a suicide vector, pJC84 (Fig. 8A) that allows for generation of untagged, in-frame deletions in the chromosome of virulent Type A strains through SacB-assisted allelic replacement. Along the allelic replacement process, PCR analysis of the targeted locus in the wild type, intermediate cointegrant and deletion mutant strains demonstrated deletion of each locus in the proper chromosomal region and loss of pJC84 sequences following the sucrose selection step (Fig. 8BCD, Supplementary Material and data not shown). To test for any intracellular growth defect of the Schu S4 mutants, BMMs were infected with either wild type or mutant strains and intracellular CFUs were enumerated. Deletion mutants in FTT0254c, FTT0297, FTT0989,

FTT1333c, FTT1392, FTT1542c and FTT1586c did not show any defect in intracellular growth in BMMs (Fig. 9A and data not shown), but the Schu S4ΔFTT0383, Schu S4ΔFTT0369c and Schu S4ΔFTT1676 mutants exhibited obvious intracellular survival or growth defects (Fig. 9A-C). While the wild type strain displayed an expected intracellular growth profile over 24 h, the number of intracellular ΔFTT0383 bacteria rapidly decreased to barely detectable levels by 16 h p.i. (Fig. 9A), indicating intracellular killing of the mutant. Comparatively, growth of the ΔFTT0383 mutant *in vitro* in modified Mueller-Hinton broth was not affected (data not shown), ruling out a global physiological defect of this strain. During the course of this study, the FTT0383 ortholog in *F. novicida* was shown to encode a transcriptional regulator, FevR, which controls virulence gene expression and is essential for intracellular growth and pathogenesis (Brotcke *et al.*, 2008). Numbers of viable intracellular ΔFTT0369c bacteria slightly increased up to 10 h p.i., then dramatically decreased by 2 Logs (Fig. 9B and F), indicating limited replication followed by intracellular killing. Compared to the parental strain that grew by 3 Logs over 16 h (Fig. 9A), ΔFTT1676 bacteria displayed an intracellular growth defect, since viable numbers remained steady during the same period before decreasing, although to a less dramatic extent than that observed with the ΔFTT0383 or the ΔFTT0369c mutants (Fig. 9C and F). Hence, deletion of either FTT0369c or FTT1676 affects intracellular proliferation and long-term survival. To confirm that the observed intracellular defects of these mutants were due to the respective single deletions of either FTT0383, FTT0369c or FTT1676, *in trans* complementation of the mutants with the respective full-length copies of the deleted gene were performed. While expression of either FTT0383 or FTT1676 under the control of the *omp26* (FTT1542c) promoter fully restored their ability to survive and grow intracellularly (Fig. 9A, C and F), the *omp26* promoter-mediated expression of FTT0369c only partially complemented the effect of the FTT0369c deletion (data not shown). Nonetheless, expression of ΔFTT0369c under its native promoter in the mutant strain (see Supplementary Material) fully restored both survival and intracellular growth (Fig. 9B and F). Altogether, these complementation studies demonstrate that the phenotypic defects of these mutants are due to their respective single gene deletion.

To further characterize these mutants, we examined their intracellular trafficking by confocal immunofluorescence microscopy using colocalization with LAMP-1-positive membranes as a readout of vacuolar versus cytosolic location (Checroun *et al.*, 2006). Unlike the wild type strain that escaped from its original phagosome by 1 h p.i. (24.4 ± 1.0% of LAMP-1-positive bacteria; Fig. 9D and F) and extensively replicated in the cytosol by 10 h p.i. (Fig. 9D and F), the ΔFTT0383 mutant remained enclosed within a LAMP-1-positive compartment (≥ 85% of bacteria) at 1 and 10 h pi (Fig. 9D and F), consistent with intracellular killing within phagolysosomes. Complementation of the FTT0383 deletion restored phagosomal escape (Fig. 9E) and cytosolic replication (Fig. 9F). Hence, deletion of the FTT0383 locus abolishes Schu S4 ability to escape from its original phagosome, survive and replicate intracellularly, consistent with results obtained with *F. novicida* (Brotcke *et al.*, 2008). By contrast, ΔFTT0369c bacteria showed phagosomal escape kinetics similar to wild type organisms, although a small fraction of bacteria (< 20%) localized to LAMP-1-positive vacuoles after 4 h p.i. (Fig. 9D). At 10 h pi., ΔFTT0369c bacteria showed limited intracellular growth by microscopy (Fig. 9F), consistent with viable numbers of intracellular bacteria (Fig. 9B). Complementation of the mutant with a full-length copy of FTT0369c restored intracellular growth (Fig. 9F) and did not affect the kinetics of phagosomal escape (Fig. 9E), demonstrating that deletion of the FTT0369c locus mostly affects cytosolic proliferation. Deletion of the FTT1676 locus decreased the ability of bacteria to rapidly escape from their original phagosome, since 60.5 ± 1.1% and 21 + 3.5% of bacteria colocalized with LAMP-1 at 1 and 4 h pi, respectively, yet the majority reached the cytosol afterwards (Fig. 9D and F). Although mostly cytosolic from 4 h pi, ΔFTT1676 bacteria did not undergo significant replication (Fig. 9C), despite some patterns of limited growth at 10 h

pi (Fig. 9C and F). Complementation of the mutant with full-length FTT1676 restored phagosomal escape and intracellular growth to wild type levels (Fig. 9E and F), indicating that the product of the FTT1676 locus is required for optimal phagosomal escape and mostly for cytosolic replication. Taken together, these results identify FTT0383 (*fevR*), FTT0369c and FTT1676 as novel bacterial determinants of Schu S4 intracellular pathogenesis.

To extend these findings, we tested whether deletion of either FTT0383, FTT0369c or FTT1676 affects *in vivo* virulence of Schu S4. Compared to intranasal or intradermal infections of BALB/cJ mice with Schu S4, which caused 100% lethality by day 5 p.i., infections with either the ΔFTT0383 or the ΔFTT0369c mutants led to 100% survival up to 30 days p.i., regardless of the route of inoculation (Fig. 10A and B), and no viable mutants could be recovered from any organ at this time (data not shown). Similarly, intradermal and intranasal infections with the ΔFTT1676 mutant led to 100 and 80% survival, respectively (Fig. 10A and B), and morbidity in mice infected intranasally was protracted. Hence, deletion of either FTT0383, FTT0369c or FTT1676 abolishes Schu S4 virulence in mice, demonstrating that these loci encode virulence factors of this pathogen. Interestingly, the intracellular defects of the FTT0369c and FTT1676 mutants - impaired cytosolic replication - correlated with the expression profiles of the deleted genes, since both FTT0369c and FTT1676 were maximally expressed during the cytosolic phase (Fig. 7A). Such a correlation was less obvious for FTT0383, probably due to its pleiotropic role as a transcriptional regulator (Brotcke *et al.*, 2008). Nonetheless, our results associate a gene function with its timed intracellular expression, endorsing transcriptional profiling to identify genes required at specific stages of the *Francisella* intracellular cycle.

In this study, we have established the intracellular transcriptome of a highly virulent strain of *F. tularensis* during its infection cycle within murine primary macrophages. The kinetic nature of our analysis has revealed key aspects of the intracellular biology of this pathogen, which effectively adapts its genetic response to its particular intracellular location. Although regulators of *Francisella* virulence gene expression have been characterized, such as MglA (Baron *et al.*, 1998, Brotcke *et al.*, 2006, Charity *et al.*, 2007), SspA (Charity *et al.*, 2007) and FevR (Brotcke *et al.*, 2008), further studies are required to better understand the regulatory networks that respond to intracellular cues and control expression of *Francisella* genes required for intracellular pathogenesis. Nonetheless, our findings illustrate the high degree of adaptation of *Francisella* to the macrophage environment, a feature that undoubtedly contributes to its high infectivity and virulence. Importantly, we have used the *Francisella* intracellular transcriptome data to confirm previously identified and discover novel virulence determinants of this pathogen. Expression profiles of the FPI genes, which encode for a major virulence determinant of *Francisella*, revealed early and late induction events, a finding consistent with induction of FPI proteins during the early phagosomal stage (Chong *et al.*, 2008), implying additional intracellular roles for the FPI. Furthermore, we have deleted a series of upregulated hypothetical functions and found that 3 out of 10 deletions caused intracellular defects in our BMM infection model. Surprisingly, we could not reproduce the intracellular growth defect observed upon deletion of the FTT0989 locus in *F. novicida* (Brotcke *et al.*, 2006). This limited number of intracellular defect-causing mutations suggests that either not all genes upregulated during the intramacrophagic cycle are essential, or that such genes may be required under conditions that were not reproduced in our infection model. For example, it remains possible that the initial infectious cycle within macrophages induces genes required at a subsequent stage of the infectious process that cannot be mimicked *in vitro*. Mouse infections with these mutants are underway to address this hypothesis, which is supported by the recent identification of the *F. novicida* ortholog of FTT1392 (FTN_1355) as required for proliferation in the liver of infected mice (Kraemer *et al.*, 2009). Nonetheless, deletion of the Schu S4 ortholog of the *F. novicida* FevR transcriptional regulator (Brotcke *et al.*, 2008) showed that this upregulated gene is

essential for intracellular survival and *in vivo* virulence of Schu S4. Given the strong defects caused by this mutation, Schu S4 FevR likely fulfills the same function as its *F. novicida* ortholog (Brotcke *et al.*, 2008), making it a key regulator of virulence in highly virulent strains. Furthermore, we have identified two novel factors required for intracellular proliferation and *in vivo* virulence that are encoded by the FTT0369c and FTT1676 loci. These genes are specific to the *Francisella* genus and their sequence is highly conserved between subspecies. While FTT0369c encodes a Sel1 family tetratricopeptide repeat-containing protein and has not previously been identified as a virulence gene, FTT1676 possibly encodes an outer membrane protein that has been shown to be required in LVS for mouse lung infection (Su *et al.*, 2007), consistent with an important role in the pathogenesis of *Francisella*. Future studies will address how the products of both genes contribute to intracellular proliferation and virulence.

Experimental Procedures

Bacterial strains and culture conditions

The prototypic Type A virulent strain, *F. tularensis* subsp. *tularensis* Schu S4 was obtained from Rick Lyons (University of New Mexico, Albuquerque, USA). Schu S4 was grown on cysteine heart agar supplemented with 9% heated sheep blood (CHAB) plates or modified Mueller-Hinton (MMH) agar plates [Mueller-Hinton medium supplemented with 0.1% glucose, 0.025% ferric pyrophosphate and 2% IsoVitaleX (Becton Dickinson, Cockeysville, MD)] for 3 days at 37°C under 7% CO_2. Immediately prior to infection of BMMs, a few colonies from a freshly streaked CHAB plate were resuspended in Tryptic-Soy broth supplemented with 0.1% L-cysteine and OD_{600nm} was measured to estimate bacterial numbers. Schu S4 liquid cultures were performed in MMH broth. For animal infections, bacteria were cultured in MMH broth at 37°C with constant shaking overnight, aliquoted into 1 ml samples, frozen at -80°C and thawed just prior to use. Frozen stocks were titered by enumerating viable bacteria from serial dilutions plated on MMH agar plates. All manipulations of *F. tularensis* strain Schu S4 were performed in a Biosafety Level 3 facility according to standard operating procedures approved by the Rocky Mountain Laboratories Institutional Biosafety Committee.

Allelic replacement in *F. tularensis* Schu S4

To generate in-frame deletions of specific genes in *F. tularensis* subsp. *tularensis* Schu S4, we constructed a suicide vector allowing for SacB-assisted allelic replacement in *Francisella*, named pJC84. To engineer pJC84, the ampicillin resistance gene *bla* from pJC80 (Celli *et al.*, 2005) was removed by inverse PCR using primers JC427 and JC428 (Supplementary Material, Table S2), digestion with *Aat*II and religation. A 920 bp region upstream of the *Bacillus subtilis sacB* gene in pJC80 was subsequently removed from the ligation product by a second inverse PCR using primers JC418 and JC420 (Supplementary Material, Table S2), to remove the *sacB* promoter region. The resulting PCR fragment was digested with *Nhe*I and *Sal*I. Independently, a ~ 350 bp fragment carrying the *Francisella groEL* promoter region was PCR amplified from pFNLTP *gro-gfp* (Maier *et al.*, 2004) using primers JC414 and JC415 (Supplementary Material, Table S2) and the kanamycin resistance encoding gene *aph* was PCR amplified from pBBR1-MCS2 (Kovach *et al.*, 1994) using primers JC416 and JC417 (Supplementary Material, Table S2) and fused together by overlap extension PCR (Horton *et al.*, 1989) using primers JC414 and JC417. The resulting 1150 bp fragment was digested with *Nhe*I and *Sal*I and ligated into the similarly digested pJC80 derivative to create pJC84. pJC84 (3775 bp, Fig. 8A) was fully sequenced and carries a bi-cistronic *aph-sacB* region under the control of the *Francisella groEL* promoter region, a feature essential to the proper expression of genes in *Francisella* (Gallagher *et al.*, 2007), a multiple cloning site with 6 unique restriction sites (Fig. 8A), and the origin of replication

ori from pSP72 (Promega) for cloning and propagation in *Escherichia coli*. The pJC84 sequence data has been submitted to the GenBank database under the accession number FJ155667.

Deletion constructs of the FTT0369c, FTT0383, FTT1542c and FTT1676 loci were generated as described in the Supplementary Material, and cloned into pJC84. To perform allelic replacement in the chromosome of Schu S4, electrocompetent bacteria were prepared as follows: Schu S4 was grown for 3 days on modified Mueller-Hinton agar plates at 37°C and 7% CO_2 and fresh colonies were suspended in modified Mueller-Hinton broth and grown at 37°C under agitation until the culture reached an OD_{600nm} between 0.4 and 0.5. Bacteria were collected by centrifugation at 4000 × *g* for 10 min at 20°C, washed twice with 0.5 M sucrose and concentrated 100 times in 0.5 M sucrose. Approximately 1×10^{10} bacteria were mixed with 1 μg of recombinant pJC84 plasmid DNA, pulsed (2.5 kV, 25 μF, 600W) using a BioRad GenePulser Xcell (BioRad, Hercules, CA) and immediately added to 1 ml of pre-warmed MMH broth and incubated at 37°C under agitation for 3 h, which was followed by plating on MMH plates supplemented with 10 μg/ml of kanamycin. Kanamycin-resistant colonies were tested for integration of the allelic replacement plasmid, using colony PCR with primers JC420 and JC427 (to amplify a 1.5 kb internal fragment of *sacB*) or JC589 and JC428 (to amplify a 900 bp fragment of pJC84 backbone). Independent clones were then subjected to sucrose counter selection: clones were inoculated in MMH broth and grown at 37°C under agitation up to an OD_{600nm} of 0.6. Sucrose at a final concentration of 5% was then added and cultures were incubated for an additional hour before plating serial dilutions on MMH supplemented with 8% sucrose and incubation at 37°C, 7% CO_2 for 2 days. Sucrose-resistant clones were patched on kanamycin-containing MMH plates to verify loss of the kanamycin-resistance marker, and colony PCR was performed to detect clones with allelic replacement within the correct chromosomal locus, using primers JC534 and JC535 and primers JC654 and JC655, respectively, for the FTT0383 deletion, using primers JC678 and JC679 and primers JC689 and JC690, respectively, for the FTT0369c deletion, using primers JC546 and JC625 and primers JC628 and JC629, respectively, for the FTT1542c deletion, using primers JC614 and JC615 and primers JC610 and JC613, respectively, for the FTT1676 deletion, and loss of the *sacB* gene using primers JC420 and JC427 (Supplementary Material, Table S2). Independent clones carrying the correct in-frame deletion in either FTT0383, FTT0369c, FTT1542c or FTT1676, were isolated and used for further studies. For genetic complementation of the mutants, plasmids pJC901, pJC903 and pJC904, which respectively express FTT0383 under the control of the *omp26* (FTT1542c) promoter region, FTT0369c under the control of its own promoter region, or FTT1676 under the control of the *omp26* (FTT1542c) promoter region, were constructed from pFNLTP6 (Maier *et al.*, 2004) as described in the Supplementary Material and introduced into the respective mutant strains by electroporation.

Macrophage culture and infection

Bone marrow cells were isolated from femurs of 6-10 week-old, C57BL/6J female mice (Jackson Laboratories, Bar Harbor, ME, USA) and differentiated into macrophages as described (Chong *et al.*, 2008), and replated in either 6-, 12- or 24-well cell culture-treated plates at a density of 1×10^6, 5×10^5 or 1×10^5 macrophages/well, respectively. BMM infections were performed as described (Chong *et al.*, 2008) at an appropriate multiplicity of infection (MOI) of 50, unless stated otherwise.

Determination of bacterial CFUs

The number of viable intracellular bacteria per well was determined in triplicate for each time point, as described previously (Chong *et al.*, 2008), with the exception that serial dilutions were plated on CHAB agar plates. To estimate intracellular growth rate of bacteria

within a particular time interval, CFU doubling times were established were established as described previously (Chong *et al.*, 2008) and were calculated from three independent experiments and expressed as mean ± SD.

Immunofluorescence microscopy

BMMs grown on 12 mm glass coverslips in 24-well plates were infected and processed for immunofluorescence labeling as described previously (Chong *et al.*, 2008). Primary antibodies used were mouse anti-*F. tularensis* LPS (US Biological, Swampscott, MA), and rat anti-mouse LAMP-1 (clone 1D4B, developed by J. T. August and obtained from the Developmental Studies Hybridoma Bank developed under the auspices of the NICHD and maintained by The University of Iowa, Department of Biological Sciences, Iowa City, IA 52242). Secondary antibodies were Alexa Fluor™ 488-donkey anti-mouse and Alexa Fluor™ 568-donkey anti-rat antibodies (Invitrogen). To quantify *Francisella* escape from its initial phagosome, phagosomal integrity assays were performed as described previously (Checroun *et al.*, 2006) with minor modifications (Chong *et al.*, 2008). Samples were observed on a Nikon Eclipse E800 epi-fluorescence microscope equipped with a Plan Apo 60×/1.4 objective for quantitative analysis, or Carl Zeiss LSM 510 or LSM 710 confocal laser scanning microscopes for image acquisition. Confocal images of 1024×1024 pixels were acquired and assembled using Adobe Photoshop CS.

Transmission electron microscopy

Infected BMMs on 12 mm Aclar coverslips were infected and processed as described (Chong *et al.*, 2008). Sections were viewed in a Hitachi H7500 transmission electron microscope at 80 kV. Images were acquired with a Hamamatsu 2K × 2K bottom mount AMT digital camera (Advanced Microscpy Techniques, Danvers, MA) and assembled in Adobe Photoshop CS3.

Isolation and amplification of total RNA from infected BMMs

BMMs seeded in 12-well plates were infected with Schu S4 at a MOI of either 200 (0, 1, 2 and 4 h time points), 50 (8, 12 h time points) or 25 (16 and 24 h time points) as described above. The use of different MOIs in this experimental design was required to recover sufficient amount of bacterial RNA at all time points analyzed. Empirical monitoring of the infection demonstrated little changes in the timing of events in the *Francisella* intracellular cycle, suggesting that, although different MOIs were used, comparable biological samples were obtained. Time zero samples were generated by adding bacteria (MOI 200; 10^8/well) directly to BMMs that had been washed with PBS, followed by the immediate addition of lysis buffer, as described below. Uninfected controls were generated at both 0 and 24h post infection. To improve the accuracy and precision of the final measurements, 4 biological replicates at each time point were generated. Due to the number of samples that could be concurrently processed, infections were performed in separate batches. To ensure that differences between batches did not affect the final measurements, the samples were randomly assigned to batches, with the limitation that samples within one plate were grouped per time point and processed simultaneously.

At each time point, samples were washed 3 times with sterile PBS to remove residual extracellular bacteria, and both BMMs and bacteria were lysed directly in the wells by the addition of 1 ml TRIzol (Invitrogen, Carlsbad, CA) and pipetting 10 times. Samples were transferred to microtubes, 200 μl chloroform were added, vials were vortexed, and centrifuged at 16,000 × g for 15 min. The RNA-containing aqueous phase was collected from each sample and passed through a Qiashredder column (Qiagen, Valencia, CA) at 21,000 × g for 2 min to homogenize any remaining genomic DNA (gDNA) in the aqueous phase. RNA was purified using the RNeasy 96 kit (Qiagen, Valencia, CA) as described

previously (Virtaneva *et al.*, 2005). RNA quality was verified on Agilent 2100 Bioanalyzer using the Pico analysis kit (Agilent Technologies, Palo Alto, CA). Contaminating gDNA was removed by DNase I treatment (DNA-free™, Applied Biosystems, CA) as described previously (Virtaneva *et al.*, 2005). During processing, all the 40 samples were randomized in 96-well plates in order to avoid any confounding due to well location, time-point, or biological replicate batch and minimize error due to plate edge effects and fluid transfers.

Because not all samples contained sufficient amounts of bacterial RNA to warrant direct hybridization on Affymetrix DNA GeneChips, an RNA amplification step was introduced as follows: all RNA samples that were generated from *F. tularensis* SchuS4-infected and non-infected BMMs were randomized on a single 96-well plate and the MessageAmp™ II-Bacteria kit (Ambion, Foster City, CA) was used to amplify 0.5 to 1 μg of mixture of *F. tularensis* and BMM RNAs according to manufacturer's instructions. Briefly, RNAs were concentrated to 5 μl, denatured for 10 min at 70°C, polyadenylated using *E.coli* polyA polymerase for 15 min at 37°C, and reverse transcribed for 2 h at 42°C using ArrayScript and polydT primer with a T7 tail. Second strand synthesis was performed immediately after first strand cDNA synthesis for 2 h at 16°C. Purified cDNA was mixed with 75 nmol of biotin-16-UTP (Roche Applied Science, Mannheim, Germany) and concentrated to 18 μl. Biotin-labeled complementary pathogen-host RNA was amplified at 37°C in an overnight 40 μl *in vitro* transcription reaction. The amount of target consisting of macrophage and *F. tularensis* cRNAs was determined by Absorbance measurements at 260 nm. The quality and the size of the amplified targets were determined on a Agilent 2100 Bioanalyzer using the Pico analysis kit (Agilent Technologies, Palo Alto, CA). The amount of *F. tularensis* cRNA was estimated by quantitative RT-PCR of the FTT0243 locus, as described below, using a standard curve method (Applied Biosystems, Foster City, CA). *F. tularensis* RNA extracted from a bacterial suspension in TSB-C was used for the RNA standard curve.

DNA microarray hybridization and analysis

An estimated 1 μg of *F. tularensis* cRNA was fragmented to 20-100 bp in size. cRNA targets were biotinylated according to the manufacturer's instructions and hybridized to a custom Affymetrix GeneChip (RMLchip2a520312F) containing 1,933 probe-sets, among which 1,581 probe-sets were derived from the annotation of the *F. tularensis* subsp. *tularensis* SchuS4 genome (NC_006570) and 352 additional probe-sets from the *F. tularensis* subsp. *holarctica* LVS strain were derived from an annotation of the LVS genome sequence (NC_007880) by Integrated Genomics. Each sample was added to standard Affymetrix hybridization master mix (2× Hybridization Buffer, B2 Control Oligo, Herring Sperm DNA, BSA, and 1× Hybridization spike with BioB, BioC, BioC, and Cre DNAs) and applied to the chip for an overnight hybridization at 40°C. Upon completion of the fluidic process, the Affymetrix 7Gplus GeneChip scanner (Affymetrix, Santa Clare, CA) was used to scan each chip and create the image files (dat). Affymetrix GeneChip Operating Software (GCOS v1.4, http://www.affymetrix.com) was used to perform the preliminary analysis of the custom chips. All *.cel files, representing individual replicates, were scaled to a trimmed mean of 500 using a scale mask consisting of the *F. tularensis* probe sets to produce the *.chp files. A pivot table with all samples was created including calls, call p-value and signal intensity for each gene. Signals from the non-infected control samples indicated that 17 Schu S4 probe-sets out of 1,581 potentially cross-hybridized with host RNA (with at least 4 present calls out of 8) and were therefore not considered as biologically significant. The pivot table was then imported into GeneSpring GX 7.3 (http://www.chem.agilent.com), where hierarchical clustering (condition tree) using a Pearson correlation similarity measure with average linkage was used to verify that biological replicates grouped together. A separate analysis was performed from the *.cel files by directly importing the files into Partek Genomics Suite software (v6.3, 6.07.0730, Partek Inc. Saint Louis, Mo.) and running

the quantile normalization without background correction to produce a PCA plot. Two samples were declared outliers based upon the quality of signal produced from the total present calls and the scale factor not grouping with the same time points. In order to create a balanced comparison, only three replicates were used for each time point. An ANOVA was formulated from this normalization process to generate p-values from the False Discovery Rate (FDR) report, and SAM (Significance Analysis of Microarrays, (Tusher *et al.*, 2001)) was also performed.

Taqman® Real Time-PCR analysis

In order to validate DNA microarray data, mRNAs from 15 selected *Francisella* genes were quantified using TaqMan® Real Time PCR analysis (Q-PCR). Remaining RNAs from either uninfected or Schu S4-infected BMMs were randomly distributed in a 96-well plate and subjected to cDNA synthesis and purification as previously described (Virtaneva *et al.*, 2005). Briefly, 4.5 μg of random primers (Invitrogen) were annealed (10 min at 70°C, 10 min at 25°C) to remaining RNA. First-strand cDNA was synthesized with 25 U/ml SuperScript™ III (Invitrogen) in the presence of 0.5 mM dNTPs, 0.5 U/ml SUPERaseIn™ RNase inhibitor (Ambion) and 10 mM dithiothreitol (DTT) for 10 min at 25°C, 60 min at 37°C, 60 min at 42°C, 10 min at 70°C. RNA was removed by alkaline hydrolysis in 1 N NaOH (30 min at 65°C), neutralized with 1 N HCl, prior to cDNA purification using QiaQuick-96 (Qiagen, Valencia, CA) according to the manufacturer's recommendations, except that an additional 10 min centrifugation was performed to remove traces of ethanol. Quantitative PCR was performed as previously described (Virtaneva *et al.*, 2005). All Q-PCR reactions were prepared using Biomek Nx (Beckman-Coulter, Fullerton, CA) robotics to minimize pipetting differences, and run in multiplex format on a 7900HT ABI TaqMan instrument (Applied Biosystems, Foster City, CA). Briefly, Platinum Q-PCR SuperMix-UDG RT-PCR reactions (Invitrogen) were carried out in a 20 μl reaction volume containing 1× Platinum Q-PCR SuperMix-UDG mix, 6 mM $MgCl_2$, 1 × ROX reference dye (1.25 mM 5-carboxy-X-rhodamine, succinimidyl ester), 300nM VIC® dye and the quencher carboxytetramethylrhodamine (TAMRA; Applied Biosystems, Foster City, CA) labeled FTT1575c (*gyrA*) probe, 200 nM target forward and reverse primers, and 300 nM of the target TaqMan® oligo at 50 °C for 2 min, 95 °C for 2 min, 55 cycles of 95 °C for 15 sec and 60 °C for 1 min. All TaqMan® probes were labeled with 6-carboxy-fluorescein (6-FAM) at the 5′ end and the quencher TAMRA at the 3′ end. All the TaqMan® Q- PCR primers and probes were designed using Primer Express v. 2.0 (Applied Biosystems). Each primer and probe was tested for cross hybridization to other *F. tularensis* and mouse genes using BLASTN. The *gyrA* gene (FTT1575c) was used in multiplex Q-PCR reactions for normalization, due to its constitutive expression both extra- and intracellularly (data not shown). ΔC_T values for each multiplex TaqMan® reaction were calculated by subtracting the C_T value of the reference gene (*gyrA*) from the C_T value of the tested gene. The median ΔC_T values for 2-3 technical replicates for each of the 3-4 biological replicates was calculated followed by transformation using the formula $2^{-\Delta CT}$ to obtain normalized expression levels. The normalized values were plotted for each time point and were fit to a curve using the cubic spline algorithm in GraphPad Prism 5.0 (GraphPad, San Diego, CA). The Affymetrix GCOS software was used to interpret Affymetrix GeneChip results, and the MAS5 algorithm was used in construction of gene expression levels for the genes of interest in Q-PCR correlation. GraphPad Prism 5.0 software (GraphPad, San Diego, CA) was used to calculate the correlation of MAS5 and TaqMan® results. The correlation of log 2(MAS5) values and Q-PCR ΔC_T values was significant with $P<0.0001$.

Intracellular expression of FPI proteins

To examine the expression of FPI proteins by intracellular bacteria, BMMs were infected with *Francisella* strains at a MOI of either 200 (0, 1, 2 and 4h time points) or 50 (8, 12, 16

and 24h time points). At each time-point, cells were washed three times with PBS and lysed in sterile distilled water to release intracellular bacteria. An aliquot was used to enumerate bacteria by CFU analysis, and the remaining volume was spun down at 16,100 × g for 5 min, 4°C to pellet bacteria. Bacterial pellets were further processed for Western blotting as described previously (Chong *et al.*, 2008). Samples were normalised to CFU equivalents.

Animal infections

Groups of ten 6-8 week-old BALB/cJ mice (Jackson Laboratories) were infected with the indicated wild type or mutant strains of *F. tularensis* Schu S4 via intranasal and intradermal routes for survival studies. Immediately prior to infection, a stock vial of bacteria was thawed and serially diluted in PBS to the appropriate bacterial density. Mice were anesthetized intraperitoneally (i.p.) with 100 μl of a 12.5 mg/ml ketamine + 3.8 mg/ml xylazine solution. For intranasal infections, approximately 10 CFU in 25 μl of PBS was administered to the nares of each mouse. This dose routinely results in 100% lethality with 5 days of infection with wild type Schu S4. For intradermal infections, mice were injected between the dermal sheets of the ear pinna with approximately 50 CFU of Schu S4 in 10 μl PBS. This dose routinely results in 100% lethality within 5 days of infection with wild type Schu S4. Actual doses were confirmed by plating the inoculum on modified Mueller Hinton (MMH) agar plates. Animals were monitored twice daily for signs of morbidity and euthanised when moribund. All animal infections were performed at Biosafety Level-3 and approved by the Rocky Mountain Laboratories Animal Care and Use Committee.

Supplementary Material

Refer to Web version on PubMed Central for supplementary material.

Acknowledgments

We are grateful to Rick Lyons and Francis Nano for the gift of strains and antibodies, to Leigh Knodler for critical reading of the manuscript and helpful suggestions, and to Tregei Starr for her help with generating the ΔFTT0369c mutant of Schu S4. This work was supported by the Intramural Research Program of the NIH, National Institute of Allergy and Infectious Diseases.

References

Bader MW, Navarre WW, Shiau W, Nikaido H, Frye JG, McClelland M, et al. Regulation of Salmonella typhimurium virulence gene expression by cationic antimicrobial peptides. Molecular microbiology. 2003; 50:219–230. [PubMed: 14507376]

Baron GS, Nano FE. MglA and MglB are required for the intramacrophage growth of Francisella novicida. Molecular microbiology. 1998; 29:247–259. [PubMed: 9701818]

Belland RJ, Zhong G, Crane DD, Hogan D, Sturdevant D, Sharma J, et al. Genomic transcriptional profiling of the developmental cycle of Chlamydia trachomatis. Proc Natl Acad Sci U S A. 2003; 100:8478–8483. [PubMed: 12815105]

Bergman NH, Anderson EC, Swenson EE, Janes BK, Fisher N, Niemeyer MM, et al. Transcriptional profiling of Bacillus anthracis during infection of host macrophages. Infect Immun. 2007; 75:3434–3444. [PubMed: 17470545]

Boschiroli ML, Ouahrani-Bettache S, Foulongne V, Michaux-Charachon S, Bourg G, Allardet-Servent A, et al. The Brucella suis virB operon is induced intracellularly in macrophages. Proc Natl Acad Sci U S A. 2002; 99:1544–1549. [PubMed: 11830669]

Brotcke A, Monack DM. Identification of fevR, a novel regulator of virulence gene expression in Francisella. Infect Immun. 2008

Brotcke A, Weiss DS, Kim CC, Chain P, Malfatti S, Garcia E, Monack DM. Identification of MglA-regulated genes reveals novel virulence factors in Francisella tularensis. Infect Immun. 2006; 74:6642–6655. [PubMed: 17000729]

Celli J, Salcedo SP, Gorvel JP. Brucella coopts the small GTPase Sar1 for intracellular replication. Proc Natl Acad Sci U S A. 2005; 102:1673–1678. [PubMed: 15632218]

Charity JC, Costante-Hamm MM, Balon EL, Boyd DH, Rubin EJ, Dove SL. Twin RNA polymerase-associated proteins control virulence gene expression in Francisella tularensis. PLoS Pathog. 2007; 3:e84. [PubMed: 17571921]

Chatterjee SS, Hossain H, Otten S, Kuenne C, Kuchmina K, Machata S, et al. Intracellular gene expression profile of Listeria monocytogenes. Infect Immun. 2006; 74:1323–1338. [PubMed: 16428782]

Checroun C, Wehrly TD, Fischer ER, Hayes SF, Celli J. Autophagy-mediated reentry of Francisella tularensis into the endocytic compartment after cytoplasmic replication. Proc Natl Acad Sci U S A. 2006; 103:14578–14583. [PubMed: 16983090]

Chong A, Wehrly TD, Nair V, Fischer ER, Barker JR, Klose KE, Celli J. The early phagosomal stage of Francisella tularensis determines optimal phagosomal escape and Francisella Pathogenicity Island protein expression. Infect Immun. 2008

Clemens DL, Lee BY, Horwitz MA. Virulent and avirulent strains of Francisella tularensis prevent acidification and maturation of their phagosomes and escape into the cytoplasm in human macrophages. Infect Immun. 2004; 72:3204–3217. [PubMed: 15155622]

de Bruin OM, Ludu JS, Nano FE. The Francisella pathogenicity island protein IglA localizes to the bacterial cytoplasm and is needed for intracellular growth. BMC microbiology. 2007; 7:1. [PubMed: 17233889]

Ellis J, Oyston PC, Green M, Titball RW. Tularemia. Clin Microbiol Rev. 2002; 15:631–646. [PubMed: 12364373]

Eriksson S, Lucchini S, Thompson A, Rhen M, Hinton JC. Unravelling the biology of macrophage infection by gene expression profiling of intracellular Salmonella enterica. Molecular microbiology. 2003; 47:103–118. [PubMed: 12492857]

Faucher SP, Porwollik S, Dozois CM, McClelland M, Daigle F. Transcriptome of Salmonella enterica serovar Typhi within macrophages revealed through the selective capture of transcribed sequences. Proc Natl Acad Sci U S A. 2006; 103:1906–1911. [PubMed: 16443683]

Fontan P, Aris V, Ghanny S, Soteropoulos P, Smith I. Global transcriptional profile of Mycobacterium tuberculosis during THP-1 human macrophage infection. Infect Immun. 2008; 76:717–725. [PubMed: 18070897]

Gallagher LA, Ramage E, Jacobs MA, Kaul R, Brittnacher M, Manoil C. A comprehensive transposon mutant library of Francisella novicida, a bioweapon surrogate. Proc Natl Acad Sci U S A. 2007; 104:1009–1014. [PubMed: 17215359]

Golovliov I, Baranov V, Krocova Z, Kovarova H, Sjostedt A. An attenuated strain of the facultative intracellular bacterium Francisella tularensis can escape the phagosome of monocytic cells. Infect Immun. 2003; 71:5940–5950. [PubMed: 14500514]

Golovliov I, Ericsson M, Sandstrom G, Tarnvik A, Sjostedt A. Identification of proteins of Francisella tularensis induced during growth in macrophages and cloning of the gene encoding a prominently induced 23-kilodalton protein. Infect Immun. 1997; 65:2183–2189. [PubMed: 9169749]

Gray CG, Cowley SC, Cheung KK, Nano FE. The identification of five genetic loci of Francisella novicida associated with intracellular growth. FEMS Microbiol Lett. 2002; 215:53–56. [PubMed: 12393200]

Hautefort I, Thompson A, Eriksson-Ygberg S, Parker ML, Lucchini S, Danino V, et al. During infection of epithelial cells Salmonella enterica serovar Typhimurium undergoes a time-dependent transcriptional adaptation that results in simultaneous expression of three type 3 secretion systems. Cell Microbiol. 2008; 10:958–984. [PubMed: 18031307]

Hensel M, Shea JE, Waterman SR, Mundy R, Nikolaus T, Banks G, et al. Genes encoding putative effector proteins of the type III secretion system of Salmonella pathogenicity island 2 are required for bacterial virulence and proliferation in macrophages. Molecular microbiology. 1998; 30:163–174. [PubMed: 9786193]

Horton RM, Hunt HD, Ho SN, Pullen JK, Pease LR. Engineering hybrid genes without the use of restriction enzymes: gene splicing by overlap extension. Gene. 1989; 77:61–68. [PubMed: 2744488]

Kiss K, Liu W, Huntley JF, Norgard MV, Hansen EJ. Characterization of fig operon mutants of Francisella novicida U112. FEMS Microbiol Lett. 2008

Kovach ME, Phillips RW, Elzer PH, Roop RM 2nd, Peterson KM. pBBR1MCS: a broad-host-range cloning vector. Biotechniques. 1994; 16:800–802. [PubMed: 8068328]

Kraemer PS, Mitchell A, Pelletier MR, Gallagher LA, Wasnick M, Rohmer L, et al. Genome-wide screen in Francisella novicida for genes required for pulmonary and systemic infection in mice. Infect Immun. 2009; 77:232–244. [PubMed: 18955478]

Lai XH, Golovliov I, Sjostedt A. Expression of IglC is necessary for intracellular growth and induction of apoptosis in murine macrophages by Francisella tularensis. Microb Pathog. 2004; 37:225–230. [PubMed: 15519043]

Larsson P, Oyston PC, Chain P, Chu MC, Duffield M, Fuxelius HH, et al. The complete genome sequence of Francisella tularensis, the causative agent of tularemia. Nat Genet. 2005; 37:153–159. [PubMed: 15640799]

Lauriano CM, Barker JR, Nano FE, Arulanandam BP, Klose KE. Allelic exchange in Francisella tularensis using PCR products. FEMS Microbiol Lett. 2003; 229:195–202. [PubMed: 14680699]

Lauriano CM, Barker JR, Yoon SS, Nano FE, Arulanandam BP, Hassett DJ, Klose KE. MglA regulates transcription of virulence factors necessary for Francisella tularensis intraamoebae and intramacrophage survival. Proc Natl Acad Sci U S A. 2004; 101:4246–4249. [PubMed: 15010524]

Lee BY, Horwitz MA, Clemens DL. Identification, recombinant expression, immunolocalization in macrophages, and T-cell responsiveness of the major extracellular proteins of Francisella tularensis. Infect Immun. 2006; 74:4002–4013. [PubMed: 16790773]

Lindgren H, Golovliov I, Baranov V, Ernst RK, Telepnev M, Sjostedt A. Factors affecting the escape of Francisella tularensis from the phagolysosome. J Med Microbiol. 2004; 53:953–958. [PubMed: 15358816]

Lindgren H, Shen H, Zingmark C, Golovliov I, Conlan W, Sjostedt A. Resistance of Francisella tularensis strains against reactive nitrogen and oxygen species with special reference to the role of KatG. Infect Immun. 2007; 75:1303–1309. [PubMed: 17210667]

Lindgren H, Stenman L, Tarnvik A, Sjostedt A. The contribution of reactive nitrogen and oxygen species to the killing of Francisella tularensis LVS by murine macrophages. Microbes Infect. 2005; 7:467–475. [PubMed: 15788155]

Lucchini S, Liu H, Jin Q, Hinton JC, Yu J. Transcriptional adaptation of Shigella flexneri during infection of macrophages and epithelial cells: insights into the strategies of a cytosolic bacterial pathogen. Infect Immun. 2005; 73:88–102. [PubMed: 15618144]

Ludu JS, de Bruin OM, Duplantis BN, Schmerk CL, Chou AY, Elkins KL, Nano FE. The Francisella pathogenicity island protein PdpD is required for full virulence and associates with homologues of the type VI secretion system. J Bacteriol. 2008; 190:4584–4595. [PubMed: 18469101]

Maier TM, Casey MS, Becker RH, Dorsey CW, Glass EM, Maltsev N, et al. Identification of Francisella tularensis Himar1-based transposon mutants defective for replication in macrophages. Infect Immun. 2007; 75:5376–5389. [PubMed: 17682043]

Maier TM, Havig A, Casey M, Nano FE, Frank DW, Zahrt TC. Construction and characterization of a highly efficient Francisella shuttle plasmid. Applied and environmental microbiology. 2004; 70:7511–7519. [PubMed: 15574954]

McCaffrey RL, Allen LA. Francisella tularensis LVS evades killing by human neutrophils via inhibition of the respiratory burst and phagosome escape. J Leukoc Biol. 2006; 80:1224–1230. [PubMed: 16908516]

Meibom KL, Dubail I, Dupuis M, Barel M, Lenco J, Stulik J, et al. The heat-shock protein ClpB of Francisella tularensis is involved in stress tolerance and is required for multiplication in target organs of infected mice. Molecular microbiology. 2008; 67:1384–1401. [PubMed: 18284578]

Mougous JD, Cuff ME, Raunser S, Shen A, Zhou M, Gifford CA, et al. A virulence locus of Pseudomonas aeruginosa encodes a protein secretion apparatus. Science (New York, NY. 2006; 312:1526–1530.

Nano FE, Zhang N, Cowley SC, Klose KE, Cheung KK, Roberts MJ, et al. A Francisella tularensis pathogenicity island required for intramacrophage growth. J Bacteriol. 2004; 186:6430–6436. [PubMed: 15375123]

O'Callaghan D, Cazevieille C, Allardet-Servent A, Boschiroli ML, Bourg G, Foulongne V, et al. A homologue of the Agrobacterium tumefaciens VirB and Bordetella pertussis Ptl type IV secretion systems is essential for intracellular survival of Brucella suis. Molecular microbiology. 1999; 33:1210–1220. [PubMed: 10510235]

Oyston PC, Sjostedt A, Titball RW. Tularaemia: bioterrorism defence renews interest in Francisella tularensis. Nat Rev Microbiol. 2004; 2:967–978. [PubMed: 15550942]

Pukatzki S, Ma AT, Sturtevant D, Krastins B, Sarracino D, Nelson WC, et al. Identification of a conserved bacterial protein secretion system in Vibrio cholerae using the Dictyostelium host model system. Proc Natl Acad Sci U S A. 2006; 103:1528–1533. [PubMed: 16432199]

Qin A, Mann BJ. Identification of transposon insertion mutants of Francisella tularensis tularensis strain Schu S4 deficient in intracellular replication in the hepatic cell line HepG2. BMC microbiology. 2006; 6:69. [PubMed: 16879747]

Ramakrishnan G, Meeker A, Dragulev B. fslE is necessary for siderophore-mediated iron acquisition in Francisella tularensis Schu S4. J Bacteriol. 2008

Santic M, Asare R, Skrobonja I, Jones S, Abu Kwaik Y. Acquisition of the vATPase proton pump and phagosome acidification is essential for escape of Francisella tularensis into the macrophage cytosol. Infect Immun. 2008

Santic M, Molmeret M, Abu Kwaik Y. Modulation of biogenesis of the Francisella tularensis subsp. novicida-containing phagosome in quiescent human macrophages and its maturation into a phagolysosome upon activation by IFN-gamma. Cell Microbiol. 2005a; 7:957–967. [PubMed: 15953028]

Santic M, Molmeret M, Klose KE, Jones S, Kwaik YA. The Francisella tularensis pathogenicity island protein IglC and its regulator MglA are essential for modulating phagosome biogenesis and subsequent bacterial escape into the cytoplasm. Cell Microbiol. 2005b; 7:969–979. [PubMed: 15953029]

Schnappinger D, Ehrt S, Voskuil MI, Liu Y, Mangan JA, Monahan IM, et al. Transcriptional Adaptation of Mycobacterium tuberculosis within Macrophages: Insights into the Phagosomal Environment. J Exp Med. 2003; 198:693–704. [PubMed: 12953091]

Schulert GS, Allen LA. Differential infection of mononuclear phagocytes by Francisella tularensis: role of the macrophage mannose receptor. J Leukoc Biol. 2006; 80:563–571. [PubMed: 16816147]

Shi H, Bencze KZ, Stemmler TL, Philpott CC. A cytosolic iron chaperone that delivers iron to ferritin. Science (New York, NY. 2008; 320:1207–1210.

Sieira R, Comerci DJ, Pietrasanta LI, Ugalde RA. Integration host factor is involved in transcriptional regulation of the Brucella abortus virB operon. Molecular microbiology. 2004; 54:808–822. [PubMed: 15491369]

Sieira R, Comerci DJ, Sanchez DO, Ugalde RA. A homologue of an operon required for DNA transfer in Agrobacterium is required in Brucella abortus for virulence and intracellular multiplication. J Bacteriol. 2000; 182:4849–4855. [PubMed: 10940027]

Starr T, Ng TW, Wehrly TD, Knodler LA, Celli J. Brucella intracellular replication requires trafficking through the late endosomal/lysosomal compartment. Traffic (Copenhagen, Denmark). 2008; 9:678–694.

Su J, Yang J, Zhao D, Kawula TH, Banas JA, Zhang JR. Genome-wide identification of Francisella tularensis virulence determinants. Infect Immun. 2007; 75:3089–3101. [PubMed: 17420240]

Sullivan JT, Jeffery EF, Shannon JD, Ramakrishnan G. Characterization of the siderophore of Francisella tularensis and role of fslA in siderophore production. J Bacteriol. 2006; 188:3785–3795. [PubMed: 16707671]

Tempel R, Lai XH, Crosa L, Kozlowicz B, Heffron F. Attenuated Francisella novicida transposon mutants protect mice against wild-type challenge. Infect Immun. 2006; 74:5095–5105. [PubMed: 16926401]

Tusher VG, Tibshirani R, Chu G. Significance analysis of microarrays applied to the ionizing radiation response. Proc Natl Acad Sci U S A. 2001; 98:5116–5121. [PubMed: 11309499]

Twine SM, Mykytczuk NC, Petit MD, Shen H, Sjostedt A, Wayne Conlan J, Kelly JF. In vivo proteomic analysis of the intracellular bacterial pathogen, Francisella tularensis, isolated from mouse spleen. Biochem Biophys Res Commun. 2006; 345:1621–1633. [PubMed: 16730660]

Valdivia RH, Falkow S. Bacterial genetics by flow cytometry: rapid isolation of Salmonella typhimurium acid-inducible promoters by differential fluorescence induction. Molecular microbiology. 1996; 22:367–378. [PubMed: 8930920]

Virtaneva K, Porcella SF, Graham MR, Ireland RM, Johnson CA, Ricklefs SM, et al. Longitudinal analysis of the group A Streptococcus transcriptome in experimental pharyngitis in cynomolgus macaques. Proc Natl Acad Sci U S A. 2005; 102:9014–9019. [PubMed: 15956184]

Weiss DS, Brotcke A, Henry T, Margolis JJ, Chan K, Monack DM. In vivo negative selection screen identifies genes required for Francisella virulence. Proc Natl Acad Sci U S A. 2007; 104:6037–6042. [PubMed: 17389372]

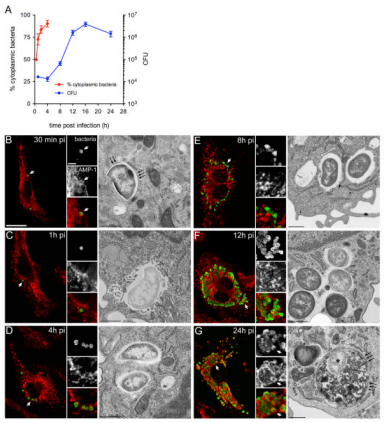

Figure 1.

Infection cycle of *F. tularensis* Schu S4 within C57BL/6J murine BMMs. BMMs were infected with Schu S4 and processed at various times post infection (p.i.) for either phagosomal integrity assay or enumeration of viable intracellular bacteria (A), or for immunofluorescence or transmission electron microscopy (B-G). (A) Phagosomal escape and intracellular growth of Schu S4 within BMMs. The percentage of cytoplasmic bacteria (red curve) was determined up to 4h p.i., as described in the Materials and Methods section, and the numbers of CFUs (blue curve) were measured up to 24 h p.i. Data are means ± SD from 3 independent experiments (phagosomal integrity assay) or from a representative experiment performed in triplicate out of 3 independent repeats (CFU). (B-G) Representative confocal and electron (TEM) micrographs of intracellular Schu S4 at 30 min (B), 1 h (C), 4 h (D), 8 h (E), 12 h (F) and 24 h p.i. (G). Bacteria (appear in green) and LAMP-1-positive membranes (appear in red) were labeled. White arrowheads indicate either regions of interest in whole images or bacteria enclosed within a LAMP-1-positive compartment (panels B and G) in insets. Black arrows in TEM micrographs indicate single or double membranes surrounding intracellular bacteria (panels B and G). The asterisk in panel G indicates a bacterium enclosed within a late autophagic-like vacuole. Scale bars, 10 and 2 μm (confocal images) or 0.5 μm (TEM images)

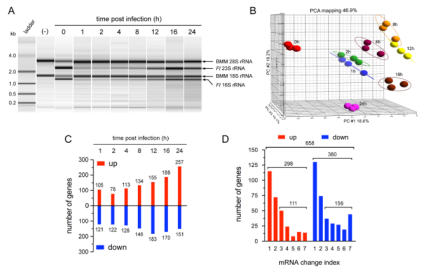

Figure 2.

Transcriptional profiling of intracellular *Francisella* (A) Representative chromatograms of total RNA isolated from either uninfected or Schu S4-infected BMMs at 0, 1, 2, 4, 8, 12, 16 and 24 h p.i., as described in the Materials and Methods section. The progressive increase in bacterial ribosomal RNAs over time mirrors the replication kinetics of intracellular bacteria (Fig. 1A). (B) Principal Component Analysis (PCA) plot showing the clustering of microarray data samples according to independent biological replicates of the same time points. PCA was performed using the Partek Genomics Suite software v6.3, as described in the Materials and Methods section. (C) Numbers of *Francisella* genes significantly up- or down-regulated at the various times p.i. Data from time zero samples was used as a baseline to determine genes whose mRNA levels varied by more than two fold. (D) Grouping of *Francisella* genes significantly up- or down-regulated according to their mRNA change index, *i.e.* the numbers of time points analyzed when expression of a given gene was significantly altered. Data from time zero samples was used as a baseline to determine genes whose mRNA levels varied by more than 2 fold. Numbers above brackets indicate the sums of genes in the included categories.

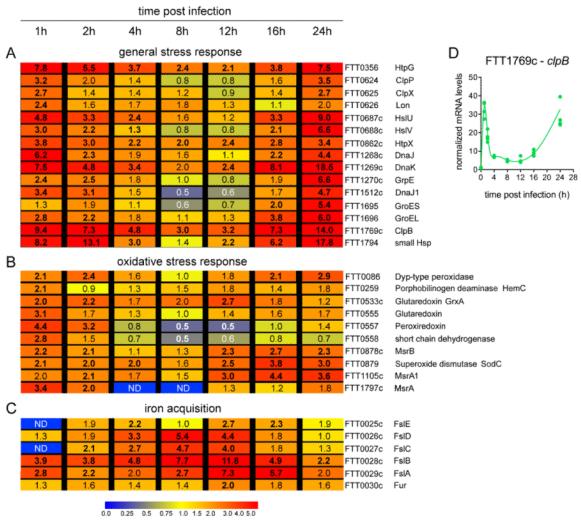

Figure 3.

Differential expression profiles of *Francisella* genes correlate with specific intracellular stages. Color-coded representations of mRNA levels of general stress response (A), oxidative stress response (B) and iron acquisition (C) genes at all time points analyzed, showing differential expression profiles of Schu S4 genes during the macrophage infection cycle. Numbers indicate fold changes in mRNA levels relative to time zero. Bold numbers correspond to significant changes in mRNA levels, as determined by statistical analyses described in the Materials and Methods section. ND indicates undetermined values due to the lack of detectable intracellular mRNA signals. Schu S4 locus tags and encoded functions are indicated. (D) Intracellular expression profile of *clpB* (FTT1769c) as determined by quantitative RT-PCR. *ClpB* mRNAs were quantified and normalized to those of the constitutively expressed *gyrA* (FTT1575c) gene.

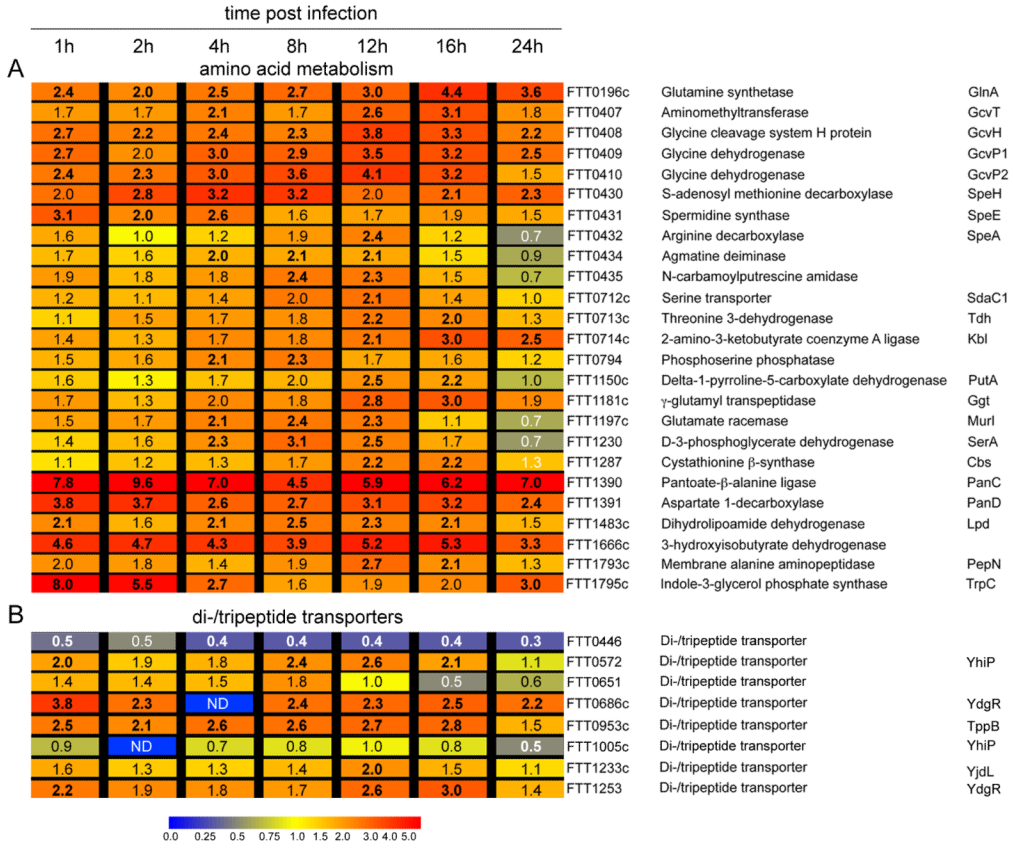

Figure 4.

Amino acid metabolism and oligopeptide transport during the *Francisella* intracellular cycle. Color-coded representations of mRNA levels of amino acid metabolism (A), and di/tripeptide transporter (B) genes at all time points analyzed. Numbers indicate fold changes in mRNA levels relative to time zero. Bold numbers correspond to significant changes in mRNA levels, as determined by statistical analyses described in the Materials and Methods section. ND indicates undetermined values due to the lack of detectable intracellular mRNA signals. Schu S4 locus tags, encoded functions and corresponding protein names or homologs are indicated.

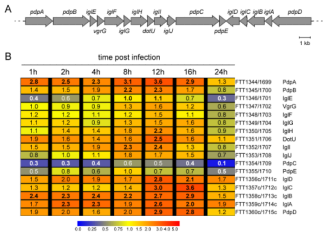

Figure 5.

Intracellular expression profiles of FPI genes by DNA Genechip analysis. (A) Schematic representation of the FPI locus in Schu S4. The gene nomenclature is according to Ludu *et al.* (Ludu *et al.*, 2008). (B) Color-coded representations of FPI gene mRNA levels during the infection cycle, showing similar expression profiles within the FPI. Numbers indicate fold changes in mRNA levels relative to time zero. Bold numbers correspond to significant changes in mRNA levels, as determined by statistical analyses described in the Materials and Methods section. Schu S4 locus tags and encoded proteins are indicated. Single probe sets for both FPI-1 and FPI-2 loci were spotted on the Genechip and identically matched with each FPI locus sequences. FPI genes are coordinately expressed and induced intracellularly.

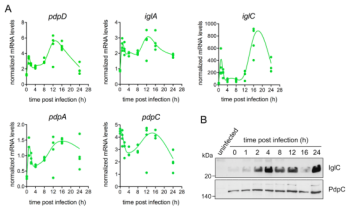

Figure 6.

Intracellular expression of FPI genes and proteins during the infection cycle. (A) Intracellular expression profiles of *pdpD*, *iglA*, *iglC*, *pdpA* and *pdpC* as determined by quantitative RT-PCR. Specific mRNAs from each gene were quantified and normalized to those of the constitutively expressed *gyrA* (FTT1575c) gene. Note the differences in the scale of normalized mRNA levels between genes. (B) Intrabacterial levels of IglC and PdpC during the intracellular cycle. BMMs were infected with Schu S4 as described in the Materials and Methods section and samples were processed for Western Blot analysis using either a monoclonal anti-IglC antibodies (upper panel) or polyclonal anti-PdpC antibodies (lower panels). Sample loading was normalized to intracellular CFU counts. Western blots are from a representative experiment out of 3 independent repeats.

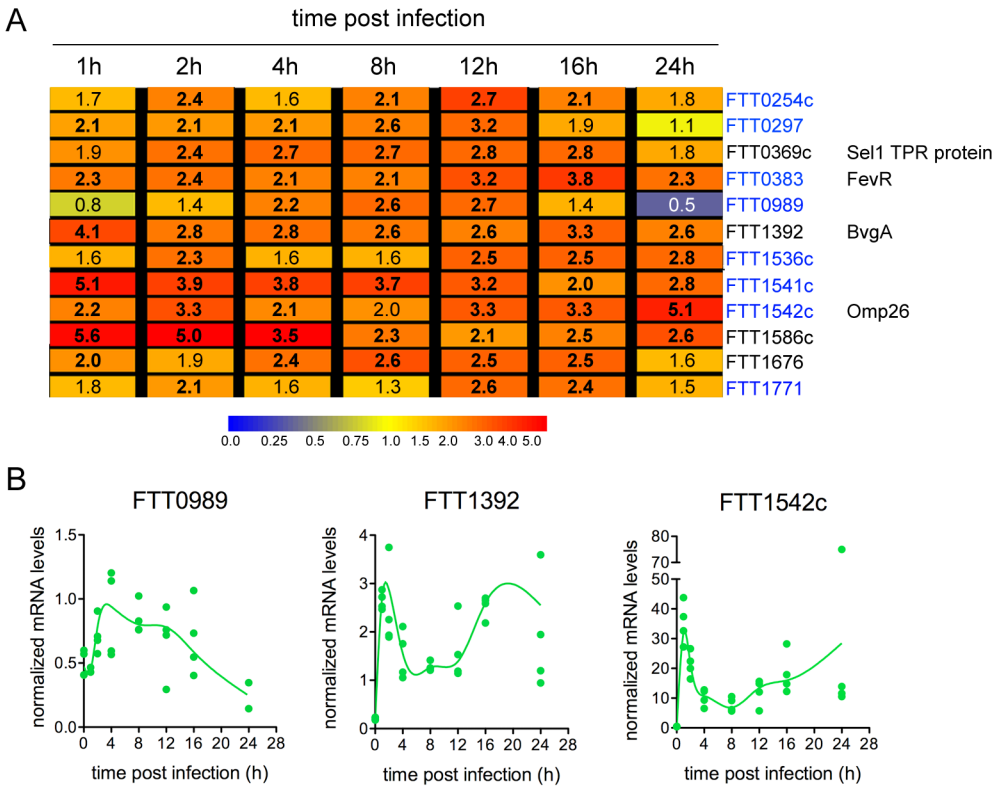

Figure 7.

Intracellular expression profiles of upregulated genes encoding hypothetical functions. (A) Color-coded representations of *Francisella* gene mRNA levels during the infection cycle, showing various profiles of intracellular upregulation. Numbers indicate fold changes in mRNA levels relative to time zero. Bold numbers correspond to significant changes in mRNA levels, as determined by statistical analyses described in the Materials and Methods section. Schu S4 locus tags and putative encoded proteins are indicated. Locus tags in blue indicate genes known to be regulated by MglA (Brotcke *et al.*, 2006). (B) Intracellular expression profiles of FTT0989, FTT1392 and FTT1542c, as determined by quantitative RT-PCR. Specific mRNAs from each gene were quantified and normalized to those of the constitutively expressed *gyrA* (FTT1575c) gene.

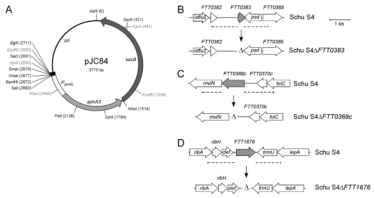

Figure 8.

SacB-assisted allelic replacement vector pJC84 and in-frame deletion of FTT0383, FTT0369c and FTT1676 in Schu S4. (A) Map of pJC84 (3775 bp; GenBank accession number FJ155667) showing the bicistronic *aph-sacB* operon under the control of the *Francisella groEL* promoter region. Unique restriction sites are indicated in black. (B) Schematic representation of the FTT0383 region of the Schu S4 chromosome before and after allelic replacement using pJC84ΔFTT0383 (see Supplementary Material). Hatched lines indicate the chromosomal regions flanking the FTT0383 locus that were used for allelic replacement. The allelic replacement was designed to preserve the integrity of the converging *psd* gene. (C) Schematic representation of the FTT0369c region of the Schu S4 chromosome before and after allelic replacement using pJC84ΔFTT0369c (see Supplementary Material). Hatched lines indicate the chromosomal regions flanking the FTT0369c locus that were used for allelic replacement. The allelic replacement was designed to preserve the integrity of the *mviN* gene located immediately downstream of FTT0369c. (D) Schematic representation of the FTT1676 region of the Schu S4 chromosome before and after allelic replacement using pJC84ΔFTT1676 (see Supplementary Material). Hatched lines indicate the chromosomal regions flanking the FTT1676 locus that were used for allelic replacement.

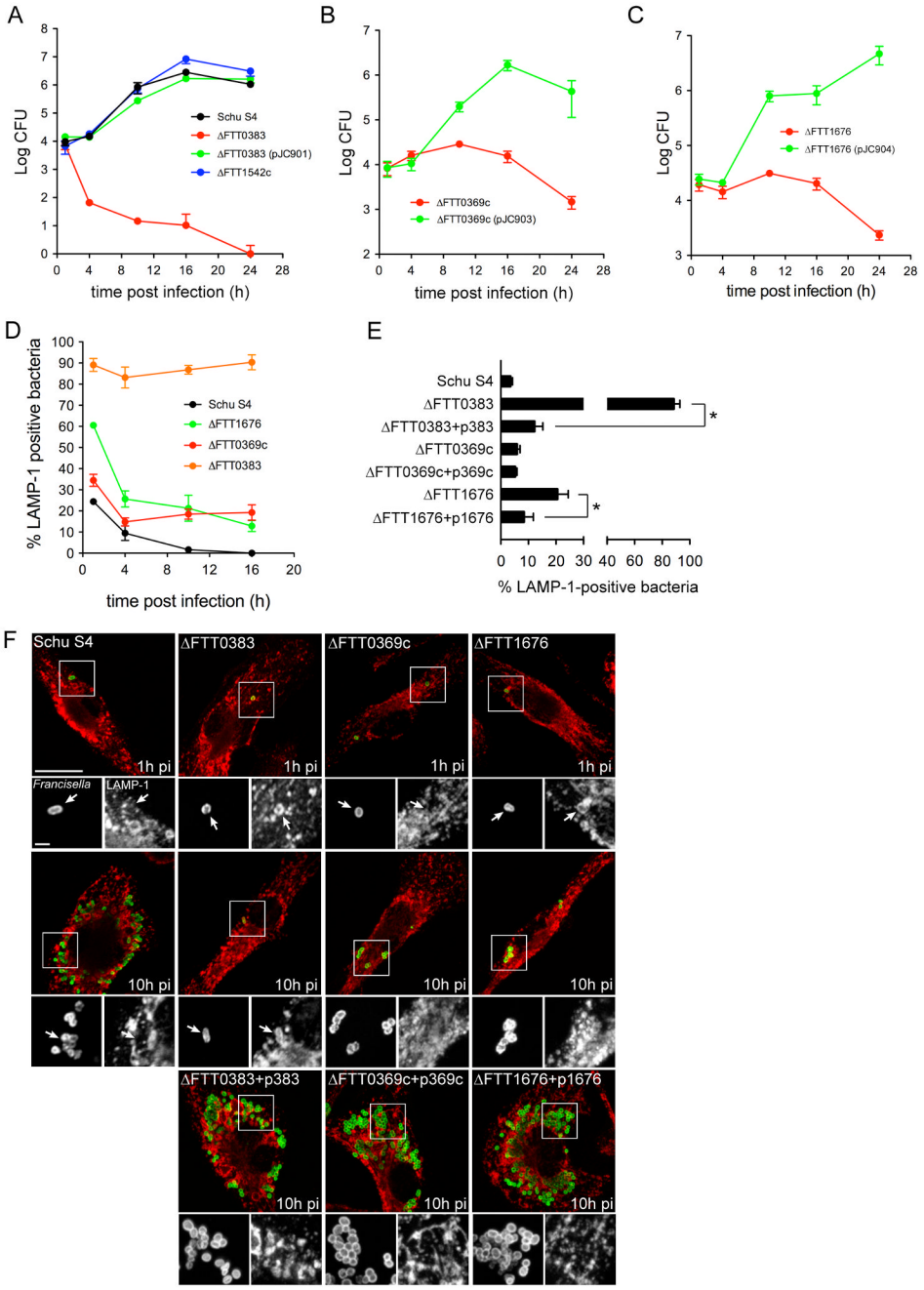

Figure 9.

Deletion of FTT0383, FTT0369c or FTT1676 affects intracellular survival or growth of Schu S4. (A) Intracellular growth of Schu S4, its isogenic ΔFTT1542c and ΔFTT0383 mutants and the complemented ΔFTT0383[pJC901] (ΔFTT0383+p383) strain in BMMs. BMMs were infected with either strains as described in the Materials and Methods section and CFUs were enumerated at various times p.i. Data are means ± SD from a representative experiment performed in triplicate out of 2 to 4 independent repeats. (B) Intracellular growth of the ΔFTT0369c and the complemented ΔFTT0369c[pJC903] (ΔFTT0369c+p369c) strains in BMMs. BMMs were infected with either strains as described and CFUs were enumerated at various times p.i. Data are means + SD from a representative experiment

performed in triplicate out of 2 independent repeats. (C) Intracellular growth of the ΔFTT1676 and *the* complemented ΔFTT1676[pJC904] (ΔFTT1676+p1676) strains in BMMs. BMMs were infected with either strains as described and CFUs were enumerated at various times p.i. Data are means + SD from a representative experiment performed in triplicate out of 2 independent repeats. (D) Quantitation of bacterial enclosure within phagosomal membranes. BMMs were infected for 1, 4, 10 or 16 h with either Schu S4 or its isogenic ΔFTT0383, ΔFTT0369c, and ΔFTT1676 mutants. Samples were processed for immunofluorescence labeling of bacteria and LAMP-1-positive membranes and numbers of bacteria enclosed within LAMP-1-positive compartments were scored. At least 100 bacteria per experiment were scored for each condition. Data are means ± SD from three independent experiments. (E) Quantitation of bacterial enclosure within phagosomal membranes at 4 h p.i. BMMs were infected for 4 h with either Schu S4 or its isogenic ΔFTT0383, ΔFTT0369c, and ΔFTT1676 mutants or the corresponding complemented strains. Samples were processed for immunofluorescence labeling of bacteria and LAMP-1-positive membranes and numbers of bacteria enclosed within LAMP-1-positive compartments were scored. At least 100 bacteria per experiment were scored for each condition. Data are means + SD from three independent experiments. Asterisks indicate a statistically significant difference ($P<0.05$, 2-tailed unpaired Student's *t*-test). (F) Representative confocal micrographs of BMMs infected for either 1 or 10 h p.i. with either Schu S4 or its isogenic ΔFTT0383, ΔFTT0369c, and ΔFTT1676 mutants (upper and middel panels), or for 10 h with the respective complemented strains ΔFTT0383+p383, ΔFTT0369c+p369c and ΔFTT1676+p1676 (lower panels). Samples were processed for immunofluorescence labeling of bacteria (appear in green) and LAMP-1-positive membranes (appear in red). Magnified insets show single channel images of the boxed region on the whole image. White arrowheads indicate bacteria of interest. Scale bars, 10 or 2 μm.

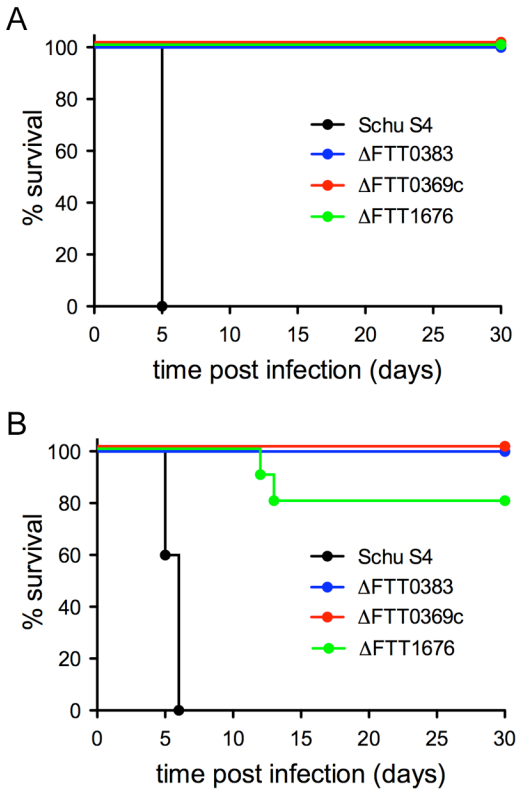

Figure 10.

The FTT0383, FTT0369c and FTT1676 loci are required for Schu S4 virulence in mice. Survival curves of BALB/cJ mice infected with either Schu S4 or its isogenic ΔFTT0383, ΔFTT0369c or ΔFTT1676 mutants after intradermal (A) or intranasal (B) inoculations. Intradermal inoculums were 30 (Schu S4), 46 (ΔFTT0383), 47 (ΔFTT0369c) and 40 (ΔFTT1676) CFUs; intranasal inoculums were 8 (Schu S4), 9 (ΔFTT0383), 13 (Δ*FTT0369c*) and 14 (ΔFTT1676) CFUs.

Table 1

F. tularensis Schu S4 genes with altered intracellular expression previously shown to be involved in intracellular growth and/or virulence

Locus tag	Gene name	Gene product	Phenotypic defect of transposon insertion mutants	Reference
Upregulated genes				
FTT0027c	*fslC*	Diaminopimelate decarboxylase	attenuation in mice (*F. novicida*)	(Weiss *et al.*, 2007)
FTT0028c	*fslB*	Multidrug resistance efflux pump	attenuation in mice (*F. novicida*)	(Weiss *et al.*, 2007)
FTT0029c	*fslA*	siderophore synthase	attenuation in mice (LVS)	(Su *et al.*, 2007)
FTT0072	*sdhC*	succinate dehydrogenase cytochrome b566	attenuation in mice (*F. novicida*)	(Weiss *et al.*, 2007)
FTT0113	*deoB*	phosphopentomutase	attenuation in mice (*F. novicida*)	(Weiss *et al.*, 2007)
FTT0209		manganese ABC transporter	attenuation in mice (LVS)	(Su *et al.*, 2007)
FTT0296	*pcp*	pyrrolidone-carboxylate peptidase	attenuation in mice (*F. novicida*)	(Weiss *et al.*, 2007)
FTT0326	*rplD*	LSU ribosomal protein L4P	attenuation in mice (*F. novicida*)	(Weiss *et al.*, 2007)
FTT0356	*htpG*	chaperone HtpG	attenuation in mice (*F. novicida*)	(Tempel *et al.*, 2006, Weiss *et al.*, 2007)
FTT0407	*gcvT*	aminomethyltransferase	attenuation in mice (*F. novicida*)	(Weiss *et al.*, 2007)
FTT0408	*gcvH*	glycine cleavage system H protein	attenuation in mice (*F. novicida*)	(Weiss *et al.*, 2007)
FTT0409	*gcvP1*	glycine dehydrogenase	attenuation in mice (*F. novicida*)	(Weiss *et al.*, 2007)
FTT0413	*glgB*	1,4-alpha-glucan branching enzyme	intracellular growth defect and attenuation in mice (LVS)	(Maier *et al.*, 2007, Su *et al.*, 2007)
FTT0414	*pgm*	phosphoglucomutase	attenuation in mice (*F. novicida*)	(Weiss *et al.*, 2007)
FTT0503c	*sucD*	succinyl-CoA synthetase alpha chain	attenuation in mice (LVS)	(Su *et al.*, 2007)
FTT0504c	*sucC*	succinyl-CoA synthetase beta chain	attenuation in mice (LVS and *F. novicida*)	(Su *et al.*, 2007, Tempel *et al.*, 2006)
FTT0610		endonuclease	intracellular growth defect (LVS)	(Maier *et al.*, 2007)
FTT0624	*clpP*	ATP-dependent protease ClpP	attenuation in mice (LVS)	(Su *et al.*, 2007)
FTT0625	*clpX*	ATP-dependent protease ClpX	attenuation in mice (LVS)	(Su *et al.*, 2007)
FTT0626	*lon*	Lon protease	attenuation in mice (LVS)	(Su *et al.*, 2007)
FTT0667		isochorismatase	attenuation in mice (*F. novicida*)	(Weiss *et al.*, 2007)
FTT0708		MFS superfamily transporter	attenuation in mice (LVS)	(Su *et al.*, 2007)
FTT0884c	*aspC1*	aspartate aminotransferase	attenuation in mice (LVS)	(Su *et al.*, 2007)
FTT0937c	*bioB*	biotin synthase	attenuation in mice (*F. novicida*)	(Weiss *et al.*, 2007)
FTT0945		para-aminobenzoate synthetase component	intracellular growth defect and attenuation in mice	(Maier *et al.*, 2007, Weiss *et al.*, 2007)
FTT1117c		isochorismatase	attenuation in mice (LVS)	(Su *et al.*, 2007)
FTT1124	*metN*	ABC transporter ATP-binding protein	intracellular growth defect (LVS)	(Maier *et al.*, 2007)
FTT1125	*metIQ*	ABC transporter permease	intracellular growth defect and attenuation in mice (LVS)	(Maier *et al.*, 2007, Su *et al.*, 2007)
FTT1269c	*dnaK*	chaperone DnaK	attenuation in mice (*F. novicida*)	(Tempel *et al.*, 2006)
FTT1344	*pdpA*	pathogenicity determinant protein PdpA	attenuation in mice (*F. novicida*)	(Weiss *et al.*, 2007)
FTT1356c	*iglD*	intracellular growth protein IglD	attenuation in mice (*F. novicida*)	(Weiss *et al.*, 2007)
FTT1357c	*iglC*	intracellular growth protein IglC	intracellular growth defect and attenuation in mice	(Su *et al.*, 2007, Weiss *et al.*, 2007)

Locus tag	Gene name	Gene product	Phenotypic defect of transposon insertion mutants	Reference
FTT1358c	*iglB*	intracellular growth protein IglB	intracellular growth defect and attenuation in mice	(Su *et al.*, 2007, Weiss *et al.*, 2007)
FTT1359c	*iglA*	intracellular growth protein IglA	intracellular growth defect and attenuation in mice	(Su *et al.*, 2007, Weiss *et al.*, 2007)
FTT1360c	*pdpD*	pathogenicity determinant protein PdpD	attenuation in mice (*F. novicida*)	(Weiss *et al.*, 2007)
FTT1392	*bvgA*	Bvg accessory factor	attenuation in mice (FTN_1355; *F. novicida*)	(Kraemer *et al.*, 2009)
FTT1676		hypothetical membrane protein	attenuation in mice (LVS)	(Su *et al.*, 2007)
FTT1696	*groEL*	chaperonin GroEL	attenuation in mice (*F. novicida*)	(Weiss *et al.*, 2007)
FTT1769c	*clpB*	chaperone ClpB	intracellular growth defect and attenuation in mice	(Gray *et al.*, 2002, Meibom *et al.*, 2008, Su *et al.*, 2007, Tempel *et al.*, 2006, Weiss *et al.*, 2007)
Downregulated genes				
FTT0051	*rbfA*	ribosome binding factor A	attenuation in mice (*F. novicida*)	(Weiss *et al.*, 2007)
FTT0138	*secE*	protein translocase subunit SecE	attenuation in mice (LVS)	(Su *et al.*, 2007)
FTT0154	*xerD*	integrase/recombinase XerD	attenuation in mice (*F. novicida*)	(Weiss *et al.*, 2007)
FTT0584		hypothetical protein	attenuation in mice (*F. novicida*)	(Weiss *et al.*, 2007)
FTT0805	*capB*	capsular polyglutamate biosynthesis protein	intracellular growth defect and attenuation in mice	(Maier *et al.*, 2007, Su *et al.*, 2007, Weiss *et al.*, 2007)
FTT0806	*capC*	capsular polyglutamate biosynthesis protein	intracellular growth defect and attenuation in mice	(Maier *et al.*, 2007, Su *et al.*, 2007, Weiss *et al.*, 2007)
FTT1234		choloylglycine hydrolase	intracellular growth defect in HepG2 cells (Schu S4)	(Qin *et al.*, 2006)
FTT1416c		hypothetical lipoprotein	attenuation in mice (LVS)	(Su *et al.*, 2007)
FTT1442c	*rpoA2*	RNA polymerase alpha chain	attenuation in mice (LVS)	(Su *et al.*, 2007)
FTT1471c	*deaD*	ATP-dependent RNA helicase	attenuation in mice (LVS)	(Su *et al.*, 2007)